

Basic Study

Distinct gut microbiomes in Thai patients with colorectal polyps

Thoranin Intarajak, Wandee Udomchaiprasertkul, Ahmad Nuruddin Khoiri, Sawanee Sutheeworapong, Kanthida Kusonmano, Weerayuth Kittichotirat, Chinae Thammarongtham, Supapon Cheevadhanarak

Specialty type: Gastroenterology and hepatology

Provenance and peer review:

Unsolicited article; Externally peer reviewed.

Peer-review model: Single blind

Peer-review report's classification

Scientific Quality: Grade B, Grade C

Novelty: Grade B, Grade B

Creativity or Innovation: Grade B, Grade B

Scientific Significance: Grade B, Grade B

P-Reviewer: Dziegielewska-Gesiak S, Poland

Received: February 21, 2024

Revised: April 30, 2024

Accepted: May 31, 2024

Published online: July 21, 2024

Processing time: 140 Days and 22.2 Hours



Thoranin Intarajak, Bioinformatics Unit, Chulabhorn Royal Academy, Lak Si 10210, Bangkok, Thailand

Thoranin Intarajak, Ahmad Nuruddin Khoiri, Kanthida Kusonmano, Weerayuth Kittichotirat, Bioinformatics and Systems Biology Program, School of Bioresources and Technology, and School of Information Technology, King Mongkut's University of Technology Thonburi, Bang Khun Thian 10150, Bangkok, Thailand

Thoranin Intarajak, Sawanee Sutheeworapong, Kanthida Kusonmano, Weerayuth Kittichotirat, Supapon Cheevadhanarak, Systems Biology and Bioinformatics Unit, Pilot Plant Development and Training Institute, King Mongkut's University of Technology Thonburi, Bang Khun Thian 10150, Bangkok, Thailand

Wandee Udomchaiprasertkul, Molecular Genomic Research Laboratory, Chulabhorn Royal Academy, Lak Si 10210, Bangkok, Thailand

Chinae Thammarongtham, National Center for Genetic Engineering and Biotechnology, King Mongkut's University of Technology Thonburi, Bang Khun Thian 10150, Bangkok, Thailand

Supapon Cheevadhanarak, School of Bioresources and Technology, King Mongkut's University of Technology Thonburi, Bank Khun Thian 10150, Bangkok, Thailand

Supapon Cheevadhanarak, Fungal Biotechnology Unit, Pilot Plant Development and Training Institute, King Mongkut's University of Technology Thonburi, Bang Khun Thian 10150, Bangkok, Thailand

Corresponding author: Supapon Cheevadhanarak, PhD, Associate Professor, School of Bioresources and Technology, King Mongkut's University of Technology Thonburi, 49 Soi Thian Thale 25, Bang Khun Thian Chai Thale Road, Bank Khun Thian 10150, Bangkok, Thailand. supapon.che@mail.kmutt.ac.th

Abstract**BACKGROUND**

Colorectal polyps that develop *via* the conventional adenoma-carcinoma sequence [*e.g.*, tubular adenoma (TA)] often progress to malignancy and are closely associated with changes in the composition of the gut microbiome. There is limited research concerning the microbial functions and gut microbiomes associated with colorectal polyps that arise through the serrated polyp pathway, such as hyperplastic polyps (HP). Exploration of microbiome alterations asso-

ciated with HP and TA would improve the understanding of mechanisms by which specific microbes and their metabolic pathways contribute to colorectal carcinogenesis.

AIM

To investigate gut microbiome signatures, microbial associations, and microbial functions in HP and TA patients.

METHODS

Full-length 16S rRNA sequencing was used to characterize the gut microbiome in stool samples from control participants without polyps [control group (CT), $n = 40$], patients with HP ($n = 52$), and patients with TA ($n = 60$). Significant differences in gut microbiome composition and functional mechanisms were identified between the CT group and patients with HP or TA. Analytical techniques in this study included differential abundance analysis, co-occurrence network analysis, and differential pathway analysis.

RESULTS

Colorectal cancer (CRC)-associated bacteria, including *Streptococcus gallolyticus* (*S. gallolyticus*), *Bacteroides fragilis*, and *Clostridium symbiosum*, were identified as characteristic microbial species in TA patients. *Mediterraneibacter gnavus*, associated with dysbiosis and gastrointestinal diseases, was significantly differentially abundant in the HP and TA groups. Functional pathway analysis revealed that HP patients exhibited enrichment in the sulfur oxidation pathway exclusively, whereas TA patients showed dominance in pathways related to secondary metabolite biosynthesis (*e.g.*, mevalonate); *S. gallolyticus* was a major contributor. Co-occurrence network and dynamic network analyses revealed co-occurrence of dysbiosis-associated bacteria in HP patients, whereas TA patients exhibited co-occurrence of CRC-associated bacteria. Furthermore, the co-occurrence of SCFA-producing bacteria was lower in TA patients than HP patients.

CONCLUSION

This study revealed distinct gut microbiome signatures associated with pathways of colorectal polyp development, providing insights concerning the roles of microbial species, functional pathways, and microbial interactions in colorectal carcinogenesis.

Key Words: Gut microbiome; Colorectal adenoma; Hyperplastic polyp; Full-length 16s rRNA; Microbial correlation networks; Predicted functional mechanisms

©The Author(s) 2024. Published by Baishideng Publishing Group Inc. All rights reserved.

Core Tip: This study identified gut microbiome signatures and metabolic pathways associated with two types of colorectal polyps. It is the first report of enrichment in the sulfur oxidation pathway among patients with hyperplastic polyps (HP) and the involvement of *Streptococcus gallolyticus* in the secondary metabolite biosynthesis pathway among patients with tubular adenoma (TA). Additionally, analysis of microbial associations in the gut microbiomes of HP and TA patients revealed a decrease in the co-occurrence of short chain fatty acid-producing bacteria. Conversely, there was an increase in the co-occurrence of dysbiosis and colorectal cancer-associated bacteria.

Citation: Intarajak T, Udomchaiprasertkul W, Khoiri AN, Sutheeworapong S, Kusonmano K, Kittichotirat W, Thammarongtham C, Cheevadhanarak S. Distinct gut microbiomes in Thai patients with colorectal polyps. *World J Gastroenterol* 2024; 30(27): 3336-3355

URL: <https://www.wjgnet.com/1007-9327/full/v30/i27/3336.htm>

DOI: <https://dx.doi.org/10.3748/wjg.v30.i27.3336>

INTRODUCTION

Colorectal cancer (CRC) is the third most prevalent cancer worldwide and the second leading cause of cancer-related mortality[1]. In Thailand, it is the fourth highest in terms of incidence and mortality rates; more than 20000 new cases have been reported in the 2020s[2]. The distinct molecular pathways leading to CRC are associated with various colorectal polyps. The most common pathway is the conventional adenoma-carcinoma sequence, which involves progression from tubular, tubulovillous, and villous adenomas. Another key pathway, the serrated polyp pathway, is characterized by the presence of colorectal polyps such as hyperplastic polyps (HP), sessile serrated adenoma/polyps (SSA/Ps), and traditional serrated adenoma. All the abovementioned colorectal polyps are regarded as neoplastic polyps with the potential to become malignant; they represent key phases in CRC progression[3].

The gut microbiome plays a pivotal role in connecting environmental factors to colorectal polyps because these factors are correlated with both compositional and functional changes within the collective microbial community residing in the colon. Alterations in the gut microbiome have been linked to colorectal polyps, and specific microbial species have been identified as potential drivers of oncogenesis. Microbial species commonly identified in precancerous lesions and

implicated in colorectal carcinogenesis include *Escherichia coli* (*E. coli*)[4,5], *Bacteroides fragilis* (*B. fragilis*)[6], and *Streptococcus gallolyticus*[7]. Additionally, shifts in *Fusobacterium mortiferum* and pro-inflammatory bacteria (e.g., *Bilophila* and *Desulfovibrio*), along with decreases in short chain fatty acid (SCFA)-producing bacteria such as *Faecalibacterium prausnitzii* and *Bifidobacterium pseudocatenulatum*, have been observed in adenoma patients[8,9]. Moreover, functional studies have elucidated the roles of specific microbes in colorectal polyp formation through processes such as co-metabolic dysfunction, inflammation, epigenetic alterations, and DNA damage[10,11]. Because the gut microbiome modulates the host metabolic environment, it can directly or indirectly influence mutagenesis rates, thereby influencing carcinogenesis. Importantly, gut microbiome differences have been discovered between healthy individuals and patients with serrated polyps[12,13]. It has been hypothesized that the unique microbiome alterations associated with early adenomas and premalignant colorectal polyps can serve as biomarkers for early cancer detection or the identification of individuals with a risk of colorectal polyps. Furthermore, an exploration of the microbiome alterations specific to premalignant or benign polyps would provide insights regarding the mechanisms by which specific microbes and their metabolic pathways contribute to colorectal carcinogenesis. However, there has been limited research concerning microbial alterations in colorectal polyps; substantial discrepancies in microbial markers across studies may be attributed to diverse biological factors that impact gut microbiome composition, as well as inconsistencies in microbial sequencing data processing[14, 15].

In this study, we compared gut microbiome signatures between two types of colorectal polyps: Tubular adenoma (TA, high potential for malignancy) and HP (low potential for malignancy). Our results revealed distinct gut microbiome signatures associated with each pathway of colorectal polyp development. Additionally, we identified microbes and microbial functions significantly associated with TA and HP. These findings suggest that gut microbiome signatures can serve as early biomarkers of CRC risk and help to identify potential targets for cancer prevention strategies.

MATERIALS AND METHODS

Participant recruitment and criteria

Participants in this study were volunteers who took part in the CRC Screening Development with Multiple Technologies Project 2020s, established by Chulabhorn Royal Academy in Thailand. The inclusion criteria were as follows: (1) Individuals aged 50-80 years who underwent CRC screening by colonoscopy between February 1, 2021, and June 30, 2022; (2) individuals who had not taken antibiotics within the preceding 3 mo; (3) individuals who did not use proton pump inhibitors or enemas, reported no history of constipation, or had undergone colonoscopy within the previous 1 mo; and (4) individuals who cooperated with the screening program and were willing to provide written informed consent. The exclusion criteria were as follows: (1) Incomplete clinical data; (2) loss of follow-up; (3) presence of inflammatory polyps; or (4) no stool sample collection. Each participant was recruited to take part in the study at the initial screening visit. They were interviewed by a physician, who recorded their clinical data and health history. After endoscopic examination of the large intestine, any detected polyps were removed and examined by a pathologist. In total, 152 participants were categorized into three groups based on the histopathology findings of the detected polyps: Control (CT), HP, and TA group. The CT group consisted of participants who exhibited no polyps during colonoscopy, the HP group comprised participants who had HP, and the TA group encompassed participants with at least one tubular or tubulovillous adenoma. The study protocol was approved by the Ethics Committee of Chulabhorn Research Institute and the Institutional Review Boards of Chulabhorn Royal Academy (Project Code 045/2563). Informed consent was obtained from all participants involved in the study.

Sample collection and DNA extraction

Stool samples were collected using DNA/RNA Shield Fecal Collection Tubes (Zymo Research, Irvine, CA, United States) prior to routine bowel preparation and colonoscopy. Participants were given a fecal collection kit and instructions for home stool sampling. Collected stool samples were stored at -20 °C until analysis. Microbial DNA was extracted from stool samples using the DNeasy PowerSoil Pro Kit (Qiagen, Germantown, MD, United States) in accordance with the manufacturer's protocol. The extracted DNA was quantified using a NanoDrop and the Qubit dsDNA HS Assay Kit (both from Thermo Fisher Scientific, Waltham, MA, United States). The ZymoBIOMICS Gut Microbiome Standard (Zymo Research) was utilized as the positive control for DNA extraction, full-length 16S rRNA amplification, and sequencing.

Full-length 16S library preparation and sequencing

Full-length 16S rRNA (V1-V9) was amplified using a set of barcoded primers: (27F) 5'-GCATC/barcode/AGRGTTY-GATYMTGGCTCAG-3' and (1492R) 5'-GCATC/barcode/RGYTACCTTGTTACGACTT-3'. The barcoded primer sequences were provided by PacBio. Each polymerase chain reaction (PCR) mixture consisted of 0.5 U Q5 High-Fidelity DNA polymerase (New England Biolabs, Ipswich, MA, United States), 200 µmol/L dNTPs, 0.5 µmol/L each forward and reverse primers, and 1 ng extracted DNA. PCR was performed using a thermocycler with the following protocol: 98 °C for 30 seconds; 22 cycles of 98 °C for 10 seconds, 55 °C for 30 seconds, and 72 °C for 1 minute; and 72 °C for 2 minutes. Library constructs for full-length 16S rRNA analysis were prepared using the SMRTbell Express Template Prep Kit 2.0 (PacBio, Menlo Park, CA, United States) and Sequel Binding Kit 3.0 in accordance with the manufacturer's protocol. Sequencing was performed using the PacBio Sequel I platform.

Microbiome data analysis

Gut microbiome analysis was conducted after a series of quality control steps using the FastQC[16] and MultiQC[17] pipelines. SMRT link v11.0 (PacBio) was utilized for demultiplexing and primer removal. Next, the QIIME2 (version 2023.2) pipeline[18] was used for microbiome profiling. Specifically, the q2-dada2 plugin (version 2023.2.0)[19] within QIIME2 was implemented for read denoising with the following criteria: pooling method, pseudo; minimum and maximum sequence lengths, 1000 and 1800 bases, respectively. Amplicon sequence variants (ASVs) were subjected to filtering, chimerism screening, and base correction. Taxonomic assignment was conducted using the Greengenes2 2022.10 database[20], which was trained with a naïve Bayes classifier. Common contaminants, unclassified ASVs, spike-ins, mitochondrial sequences, and chloroplast sequences were removed. Microbiome diversity and abundance were analyzed using the PhyloSeq (version 1.42.0)[21] and microbiome (version 1.20.0)[22] packages in R software[23]. Statistical analysis was conducted by the Wilcoxon and Kruskal-Wallis rank sum tests. Microbial richness and evenness were assessed *via* metrics such as the Shannon index[24], Simpson index[25], phylogenetic diversity (PD)[26], and Pielou index[27]. β -diversity was determined by Bray-Curtis distance-based principal coordinate analysis (PCoA)[28,29].

Gut microbiome signature discovery and co-occurrence network analysis

Gut microbiome signatures were identified using the linear discriminant analysis effect size (LEfSe) discovery tool[30,31]. Before data entry into LEfSe, normalization was performed by rarefaction of 13500 reads. Class comparisons were conducted using the Kruskal-Wallis test, whereas subclass comparisons were conducted with the Wilcoxon test. Both tests used a significance threshold of $P < 0.05$. Differential abundance analyses based on the negative binomial distribution were performed with the DESeq2 package (version 1.38.3)[32]. The abundances were imported into the DESeq2 package, and the Wald test was used to determine statistical significance[33]. Co-occurrence correlation analyses were carried out using FastSpar (version 0.0.10) software[34]. Correlation coefficients were averaged across five inference iterations, and P values were determined by 1000 bootstrap correlations. Correlation coefficients with P values less than 0.05 and absolute correlation values greater than 0.4 were selected for visualization in Cytoscape (version 3.10.0) software [35]. Comparisons among three networks (one network per group) were performed using the DyNet application[36] in Cytoscape. Microbial species with a rewiring metric or D_n -score of ≥ 2.0 , as well as an edge count of ≥ 4 , were regarded as rewired nodes for each dataset in comparisons between the CT and HP groups and between the CT and TA groups.

Functional pathway and enzyme commission enrichment analyses

To explore the metabolic functions and pathways of the gut microbiome in each group, PICRUSt2 software[37] was utilized to make predictions about microbial functions within metabolic pathways. The compositions of the identified microbes were aligned with the MetaCyc database[38] to obtain estimates of their metabolic functions. Statistical Analysis for Metagenomic Profiles (STAMP; version 2.1.3) software[39] was employed to detect variations in metabolic function abundance among groups using Welch's t -test[40] with a confidence interval of 0.95 and a significance threshold of $P < 0.05$. Gut microbiome contributions to specific pathways were determined by collecting pathway-associated enzyme commission (EC) numbers from MetaCyc and sorting on the basis of relative abundance.

RESULTS

Participant characteristics

In total, 440 participants were invited to participate in the CRC Screening Development with Multiple Technologies Project 2020s between February 1, 2021, and June 30, 2022; of these, 152 participants were enrolled in the experiment (Figure 1). Participants were categorized into three groups: 40 in the CT group, 52 in the HP group, and 60 in the TA group. Table 1 presents the demographic and clinical characteristics of the study participants. Participants in the HP and TA groups tended to be older than participants in the CT group. The number of women did not significantly differ among the three groups, but the CT group had the lowest number of men. Most participants in the HP group had polyps in the distal colon, whereas participants in the TA group had polyps in the distal and proximal colon.

Microbial community investigation

Data preprocessing with the QIIME2 pipeline revealed an average read length of 1452.95. The minimum and maximum sequence lengths were 1363 and 1788 bases, respectively. Supplementary Figure 1 shows the sequence length statistics and alpha rarefaction curve. Source Data Supplementary Table 1 lists the numbers of reads during the denoising process.

Microbiome diversities were compared among study groups using the Wilcoxon rank sum test and Kruskal-Wallis rank sum test. In terms of α -diversity, there were no significant differences among the CT, HP, and TA groups according to the Wilcoxon rank sum test. Analyses using the Shannon index ($P = 0.47$), PD ($P = 0.85$), Simpson index ($P = 0.42$), and Pielou index ($P = 0.72$) indicated that α -diversity did not significantly differ between the HP and CT groups (Figure 2A). Furthermore, α -diversity did not significantly differ between the CT and TA groups [Shannon index ($P = 0.38$), PD ($P = 0.75$), Simpson index ($P = 0.29$), and Pielou index ($P = 0.48$); Figure 2B].

Bray-Curtis distance-based PCoA was performed to assess β -diversity among participants in the CT, HP, and TA groups. As shown in Figure 2C and D, there were no significant differences in gut microbiome composition between the CT and HP groups or the CT and TA groups. Thus, the CT, HP, and TA groups did not demonstrate significant differences in richness and evenness at the species level.

Table 1 Participant demographic and clinical characteristics

Group	CT, n = 40	HP, n = 52	TA, n = 60
Age in years, median (range)	56 (52-59)	60 (51-71)	61 (52-71)
Sex			
Female	31 (77.5)	32 (61.5)	31 (51.7)
Male	9 (22.5)	20 (38.5)	29 (48.3)
BMI in kg/m ² , median (range)	21.7 (18-26.56)	23.4 (18.6-38.3)	24 (19-32)
Polyp location			
Proximal		6 (11.5)	21 (35)
Distal		39 (75)	22 (36.7)
Both		7 (13.5)	17 (28.3)

Data are n (%). BMI: Body mass index; CT: Control; HP: Hyperplastic polyps; TA: Tubular adenoma.

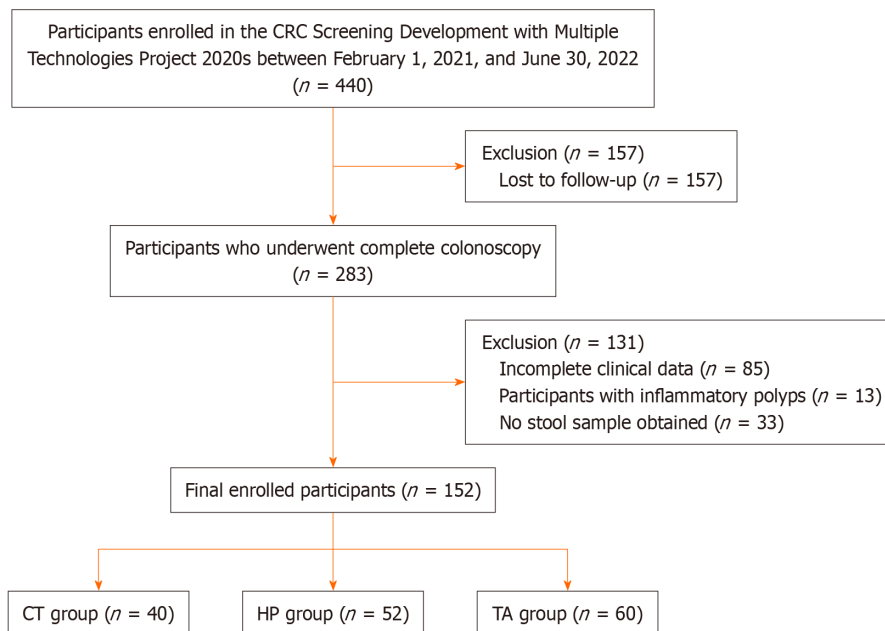


Figure 1 Flowchart of participant enrollment. CRC: Colorectal cancer; CT: Control group; HP: Hyperplastic polyps; TA: Tubular adenoma.

Groupwise comparative analyses of gut microbial species: CT vs HP and CT vs TA

To identify gut microbiome signatures that could distinguish the CT group from the HP and TA groups, we compared microbial species between the CT and HP groups, and between the CT and TA groups, using the LEfSe method and DESeq2. LEfSe, a powerful tool for the discovery of high-potential signatures, combines non-parametric standard tests for statistical significance with linear discriminant analysis (LDA). The LDA model within LEfSe identifies microbial species that are differentially abundant between groups, then estimates the effect size of each significantly different microbial species[31]. In contrast, DESeq2 utilizes a negative binomial generalized linear model to estimate log fold changes between two groups, then evaluates the significance of those changes using the Wald test[33].

LEfSe revealed that ten microbial species significantly differed between the CT and HP groups (Figure 3A, Source Data Supplementary Table 2). Among these, four microbial species were enriched in the HP group: *Blautia* A 141780 *hansenii* (*B. hansenii*), *Ruminococcus* C 58660 sp000433635, UBA9414 sp003458885, and *Veillonella* A *atypica* (*V. atypica*). Additionally, LEfSe revealed that 20 microbial species significantly differed between the CT and TA groups (Figure 3B, Source Data Supplementary Table 2). Seven microbial species were significantly enriched in the TA group, including two CRC-associated bacteria (*Bacteroides* H *fragilis* and *Clostridium* Q 134516 *symbiosum*), as well as *Bacteroides nordii* and *Clostridium* Q *fessum* (Figure 3B, Source Data Supplementary Table 2).

According to DESeq2, 22 microbial species exhibited significantly different abundances in the HP group; these included dysbiosis and gastrointestinal diseases-associated bacteria, such as *Mediterraneibacter gnavus* (*M. gnavus*) and *Fusobacterium varium* (*F. varium*), as well as commensal and SCFA-producing bacteria (e.g., *B. hansenii*, *Butyribacter*

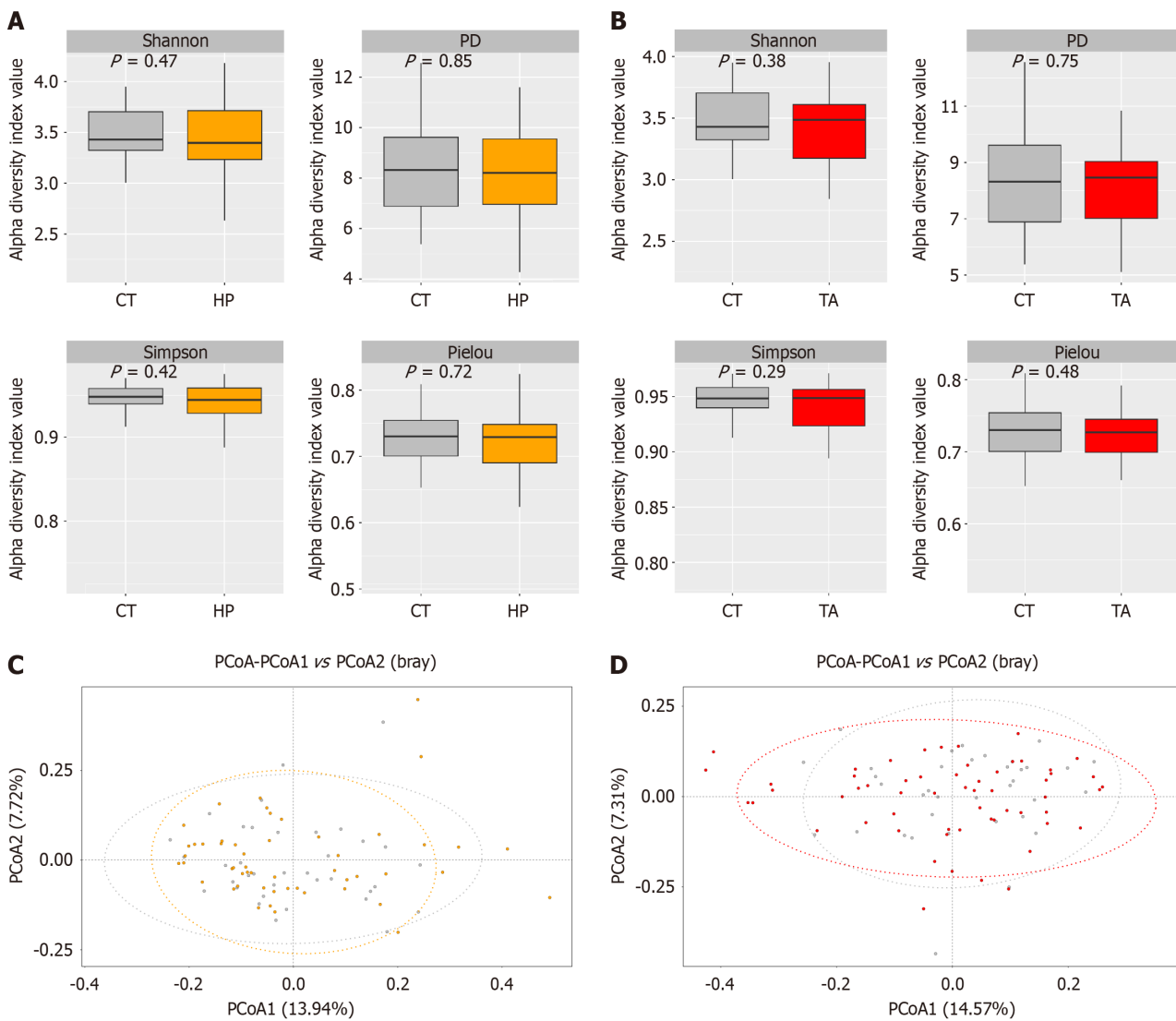
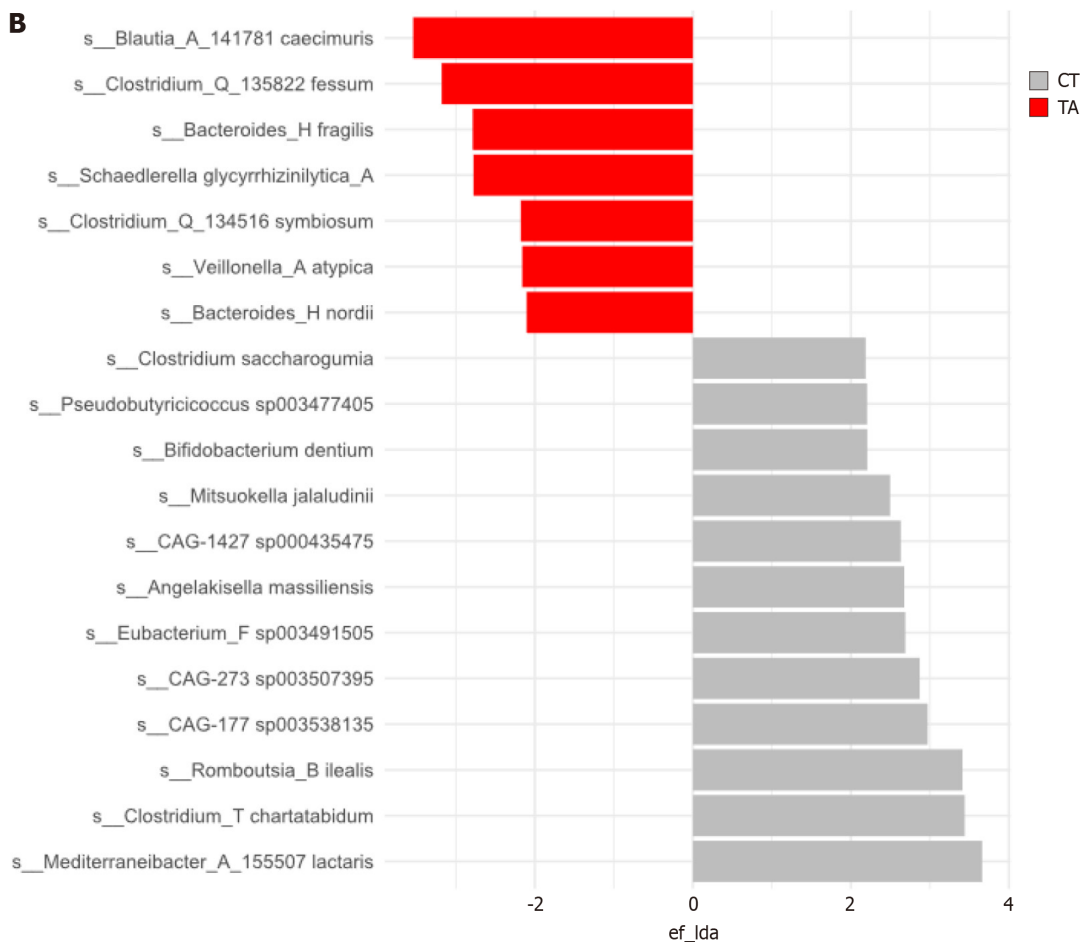
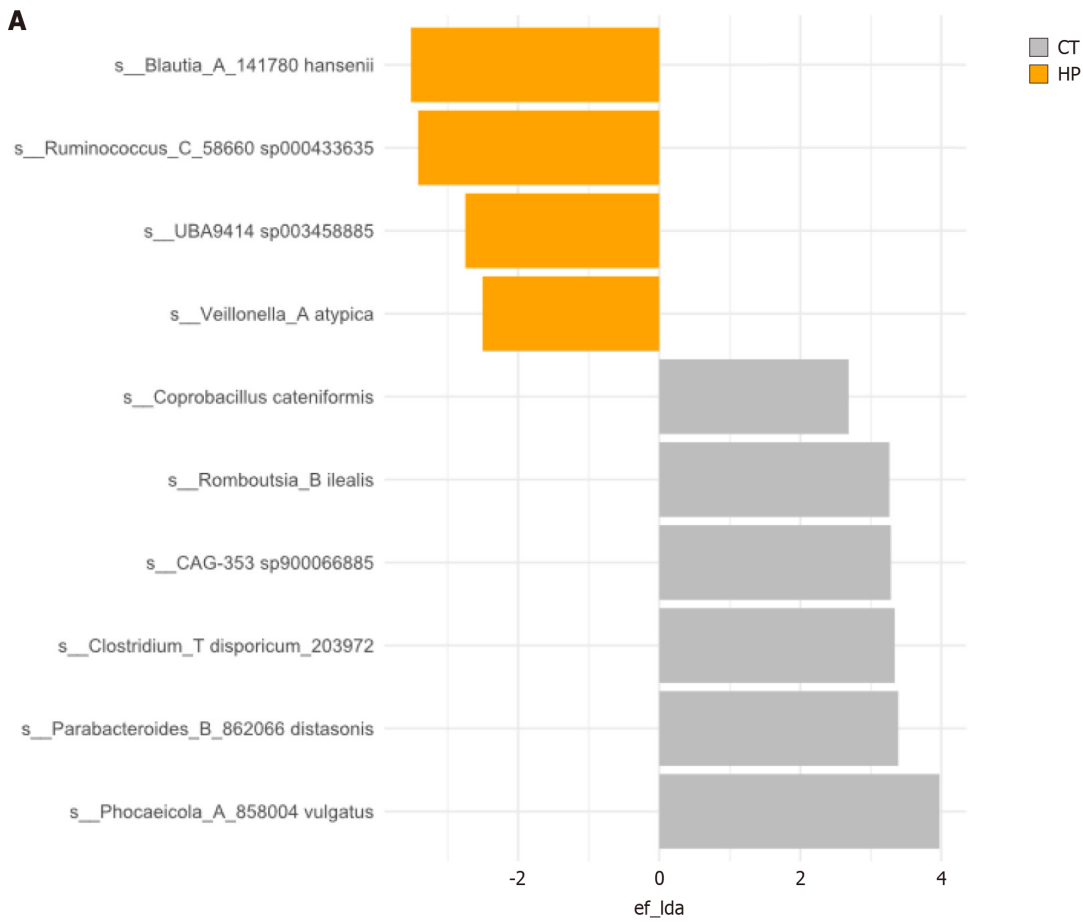


Figure 2 Microbial diversity of the gut microbiome in control, hyperplastic polyps, and tubular adenoma groups. A: Box plots show α -diversity between the control (CT) and hyperplastic polyps (HP) groups; B: Box plots show α -diversity between the CT and tubular adenoma (TA) groups; C: Principal coordinate analysis (PCoA) plots show β -diversity between the CT and HP groups; D: PCoA plots show β -diversity the CT and TA groups. PD: Phylogenetic diversity.

sp001916135, *Bifidobacterium catenulatum*, and *Faecalimonas umbilicata*) (Figure 3C, Source Data Supplementary Table 2). Additionally, 20 microbial species showed significantly different abundances in the TA group (Figure 3D), including *S. gallolyticus* (a well-known CRC-associated species), *M. gnavus*, and *F. varium*. Additionally, *V. atypica* demonstrated significantly different abundances in the HP and TA groups. *V. atypica* is commonly localized in the oral cavity and has been identified in fecal samples from older patients with CRC [41,42]. Notably, the TA group had increased abundances of well-known CRC-associated bacteria. These findings suggest that increases in *S. gallolyticus* and *B. fragilis* contribute to TA development. The findings also support the notion that patients with colorectal polyps exhibit a dysregulated microbiome characterized by high abundances of potentially pathogenic bacteria. In summary, our results imply that the identified microbial species could be used as signatures for HP and TA. We also assessed the presence of pathogenic bacteria commonly associated with CRC, such as *F. nucleatum* and *E. coli*. In this study, *F. nucleatum* and *E. coli* were not detected in the taxonomic annotation (Source Data Supplementary Table 2).

Predicted functional signatures in HP and TA groups

To identify the mechanisms by which the gut microbiome influences CRC carcinogenesis and detect biologically significant differences, we examined changes in functional composition using the MetaCyc pathway database. Compared with the CT group, the HP and TA groups had 20 and eight enriched pathways, respectively (Figure 4). Enriched pathways in the HP group included cell structure biosynthesis [e.g., peptidoglycan biosynthesis I (meso-diaminopimelate containing)]; inorganic nutrient metabolism [super pathway of sulfur oxidation (*Acidianus ambivalens*)]; fatty acid and lipid biosynthesis (e.g., CDP-diacylglycerol biosynthesis I); cofactor, carrier, and vitamin biosynthesis; carboxylic acid biosynthesis; secondary metabolite biosynthesis; tetrapyrrole biosynthesis; and amino acid biosynthesis. Secondary metabolite biosynthesis; aromatic compound degradation; cofactor, carrier, and vitamin biosynthesis; and cell structure biosynthesis were enriched in the TA group. The main differential pathways in the TA group were related to secondary



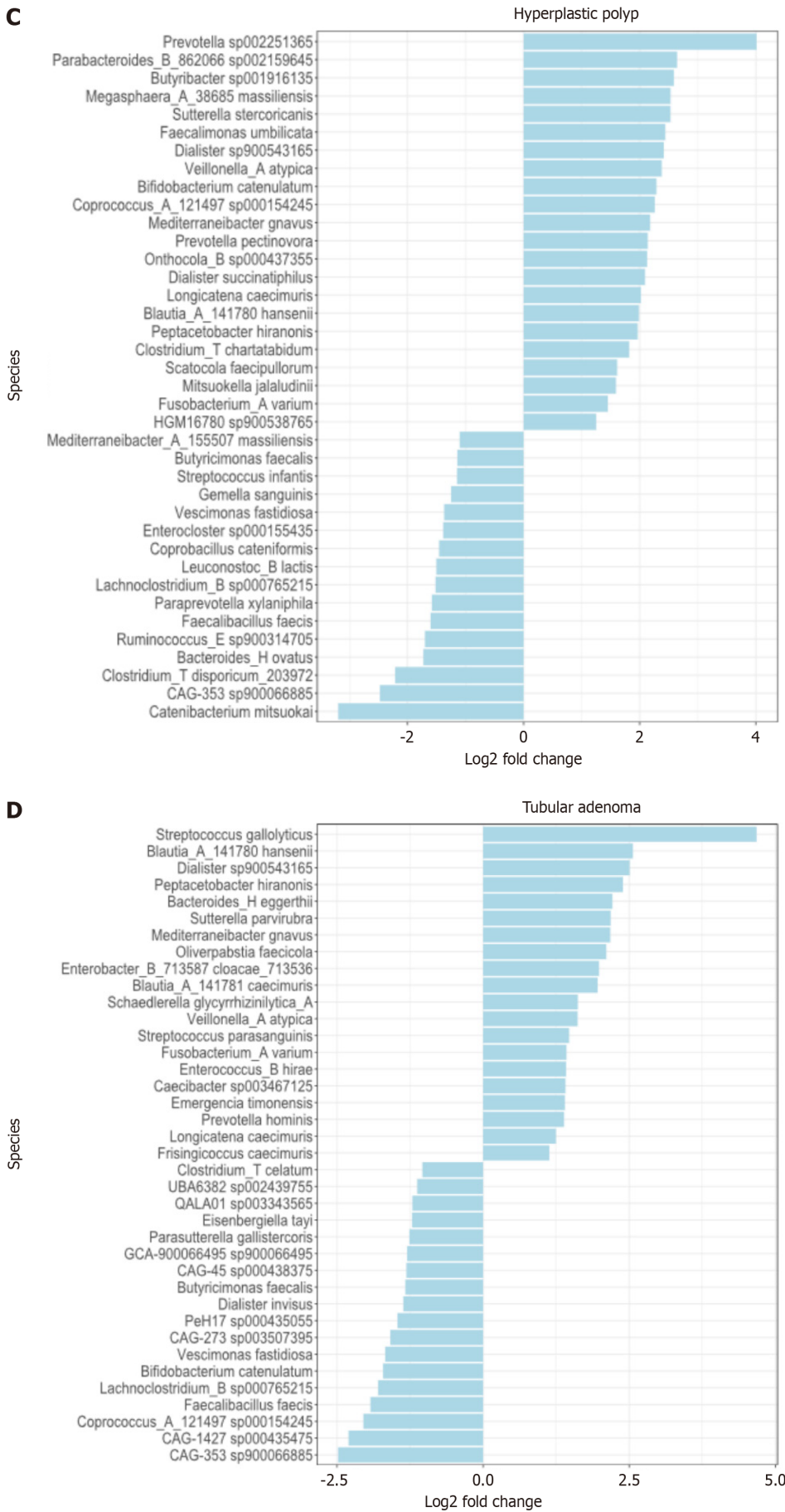


Figure 3 Linear discriminant analysis effect size and DESeq2 identified the most enriched microbial species in the control, hyperplastic

polyps, and tubular adenoma groups. A: Linear discriminant analysis (LDA) effect size (LEfSe) showed significant microbial differences between the control (CT) and hyperplastic polyps (HP) groups; B: LEfSe showed significant microbial differences the CT and tubular adenoma (TA) groups (LDA score > 2); C: DESeq2 analysis graphs illustrate the \log_2 fold differential abundances of microbial species between the CT and HP groups; D: DESeq2 analysis graphs illustrate the \log_2 fold differential abundances of microbial species between the CT and TA groups. In the graphs, \log_2 fold changes > 0 indicate an increase in the corresponding microbial species, whereas \log_2 fold changes < 0 indicate a decrease. Microbial species positioned above the zero threshold demonstrated higher relative abundance in either the HP or TA group compared to the CT group.

metabolite biosynthesis: Taxadiene biosynthesis (engineered), mevalonate pathway I (eukaryotes and bacteria), and the super pathway of geranylgeranyl diphosphate biosynthesis I (*via* mevalonate). Notably, mevalonate pathway I (eukaryotes and bacteria) overlapped between the HP and TA groups.

Next, we investigated the contributions of microbial species to the enriched pathways in the HP and TA groups. The dominant reactions in the sulfur oxidation (*Acidianus ambioalens*) pathway are adenylyl-sulfate reductase (APS reductase (EC:1.8.99.2)) and the thiosulfate dehydrogenase (quinone) pathway (EC:1.8.5.2). In the HP group, 17 and 22 microbial species contributed to the APS reductase pathway (EC:1.8.99.2) and the thiosulfate dehydrogenase (quinone) pathway (EC:1.8.5.2), respectively. *Parabacteroides* B 862066 *distasonis* (*P. distasonis*), *Bacteroides* H *thetaitaomicron* (*B. thetaitaomicron*), and *Bacteroides* H *cellulosilyticus* were the main contributors to the thiosulfate dehydrogenase (quinone) pathway. Furthermore, the APS reductase pathway was associated with *Bilophila wadsworthia* (*B. wadsworthia*) and *Desulfovibrio piger* (*D. piger*), both sulfate-reducing bacteria (SRB) (Source Data [Supplementary Table 3](#)).

In the TA group, several enzymes in enriched pathways had large contributions from *S. gallolyticus*; these enzymes included hydroxymethylglutaryl-CoA synthase (EC:2.3.3.10), mevalonate kinase (EC:2.7.1.36), phosphomevalonate kinase (EC:2.7.4.2), diphosphomevalonate decarboxylase (EC:4.1.1.33), and isopentenyl-diphosphate delta-isomerase (EC:5.3.3.2) (Source Data [Supplementary Table 4](#)). These findings suggested that the development of TA could be influenced by functional pathways associated with distinct gut microbiome signatures.

Analysis of microbial correlation networks in CT, HP, and TA groups

Microbial correlation networks and hub species were explored *via* co-occurrence network analyses that examined patterns of microbial correlation in the two colorectal polyp types. Microbial association networks were constructed for CT, HP, and TA groups using FastSpar. [Table 2](#) presents the network properties of the CT, HP, and TA groups. The CT network exhibited the largest size in terms of the numbers of nodes and edges, as well as network diameter. These findings indicated that the CT network was more extensive and complex compared with the HP and TA networks. Moreover, the CT network contained a higher number of microbial contributors compared with the HP and TA networks, suggesting that it plays a crucial role in maintaining the overall status of the system.

Nodes with a high degree (> 10) were regarded as hub species in the co-occurrence networks. In the CT network ([Figure 5A](#)), 29 hub species were identified, including *Coprococcus* A 187866 *catus* (*C. catus*), *Clostridium ramosum* (*C. ramosum*), ER4 sp000765235, *Lawsonibacter* sp000177015, *Sellimonas intestinalis*, *Blautia* A 141781 *caecimuris* (*B. caecimuris*), *Blautia* A 141781 *massiliensis* (*B. massiliensis*), and *Anaerobutyricum soehngenii* (*A. soehngenii*) ([Supplementary Figure 2A](#)). In the HP network ([Figure 5B](#)), 27 hub species were identified, including *M. gnavus*, *C. ramosum*, *Dysosmobacter* sp000403435, *Agathobacter rectalis* (*A. rectalis*), *B. hansenii*, *Clostridium* Q 135853 *saccharolyticum* A, *B. caecimuris*, *Enterocloster bolteae* (*E. bolteae*), *Dorea* A *formicigenerans* (*D. formicigenerans*), and *B. thetaitaomicron* ([Supplementary Figure 2B](#)). In the TA network ([Figure 5C](#)), 19 hub species were identified. *Blautia* A 141781 *obeum* had the highest node degree, followed by *E. bolteae*, *Dorea* A *longicatena*, *Clostridium* AQ *innocuum*, *Dysosmobacter* sp000403435, *M. gnavus*, *D. formicigenerans*, *C. catus*, *C. ramosum*, and *B. caecimuris* ([Supplementary Figure 2C](#)). Furthermore, the CT, HP, and TA networks contained commensal bacteria within the *Blautia* genus: *B. massiliensis*, *Blautia* A 141781 *faecis*, *Blautia* A 141780 *argi*, *B. obeum*, *B. caecimuris*, and *B. wexlerae*. Notably, *B. hansenii* was exclusively present in the HP and TA networks. Many SCFA-producing bacteria were identified as hub species, including *C. catus*, *Faecalibacterium prausnitzii* C 71358, *A. rectalis*, *Anaerobutyricum hallii*, *A. soehngenii*, and *F. umbilicata*. Some hub species were opportunistic pathogens, dysbiosis-associated bacteria, and CRC-associated bacteria, such as *E. bolteae*, *M. gnavus*, *C. symbiosum*, and *C. ramosum*.

The microbial correlation networks indicated that although many microbial interactions were present in all groups, some interactions were exclusive to one or two groups, suggesting that altered microbial interactions partly contribute to the distinct gut microbiome signatures of the HP and TA groups; these findings also highlight the potential role of the gut microbiome in promoting colorectal polyp development. Numerous microbial interactions present in the CT network were absent from the HP and TA networks. Specifically, the CT network showed unique microbial associations, such as negative interactions of *C. catus* with *Lawsonibacter* sp000177015 and *C. ramosum*. There were also positive interactions among CT-associated bacteria, such as CAG-45 sp000438375 (*Lachnospiraceae*) with *Coprococcus* A 121497 *eutactus* and CAG-353 sp900066885 (*Ruminococcaceae*). Additionally, some positive interactions between SCFA-producing bacteria such as *A. hallii* and *A. soehngenii*, and between *C. eutactus* and *Butyribacter* sp003529475, were absent from the HP and TA networks. Furthermore, the HP and TA networks exhibited specific microbial associations that were absent from the CT network, especially the interactions between commensal bacteria and SCFA-producing bacteria, as well as dysbiosis and CRC-associated bacteria. For example, positive interactions of *M. gnavus* with *B. hansenii* and *F. umbilicata* were observed. Positive interactions of *E. bolteae* with *B. hansenii*, *Ruthenibacterium lactatiformans*, and *Clostridium* Q 135853 *saccharolyticum* A, as well as positive interactions of *M. gnavus* with *Mediterraneibacter* A 155507 *torques*, *B. thetaitaomicron*, *Bacteroides caccae*, *Faecalimonas phoceensis*, and *Phocaeicola* A 858004 *vulgatus*, were exclusively present in the HP network. In contrast, positive interactions of *E. bolteae* with *B. fragilis* and *P. distasonis*; *B. fragilis* with *C. innocuum* and *C. ramosum*; and *C. ramosum* with *B. thetaitaomicron* were present in the TA network. These findings support the notion of dysbiosis

Table 2 Correlation network properties of the control, hyperplastic polyp, and tubular adenoma groups

Network properties	CT	HP	TA
Number of nodes	187	137	117
Number of edges	469	372	302
	(pos = 311, neg = 158)	(pos = 245, neg = 127)	(pos = 210, neg = 92)
Clustering coefficient	0.2	0.306	0.302
Network diameter	10	8	7
Average number of neighbors	5.613	6.698	5.650
Network density	0.035	0.064	0.055
Network centralization	0.130	0.255	0.15353

CT: Control; HP: Hyperplastic polyps; Neg: Negative; Pos: Positive; TA: Tubular adenoma.

involvement in colorectal polyp development.

To further characterize the microbial community structure and key microbial associations among patients with different types of polyps, dynamic changes in interactions between the CT and HP networks, and between the CT and TA networks, were explored *via* DyNet analyses that identified synchronized and rewired nodes across the two datasets. The rewired node score was determined by the D_n -score, which reflects the altered interactions of microbial species across the synchronized networks in the two datasets. DyNet visualization of the synchronized CT and HP networks revealed 92 rewired nodes; 70 rewired nodes were present in both datasets (Figure 6A). Similarly, the synchronized CT and TA networks exhibited 108 rewired nodes; 83 rewired nodes were present in both datasets (Figure 6B). Additionally, the synchronized networks showed seven and two rewired nodes that were exclusive to the HP and TA datasets, respectively. DyNet visualization revealed that unique rewired nodes in the HP group consisted of SCFA-producing bacteria, commensal bacteria, and CRC-associated bacteria. For example, *A. rectalis*, *Ruminococcus D bicirculans*, *Blautia A 141780 stercoris*, *Eubacterium I ramulus*, and *S. gallolyticus* were identified as unique rewired nodes in the HP group. In contrast, *A. rectalis* and *Megamonas funiformis* were identified as unique rewired nodes in the TA group. Many interactions involving rewired nodes exclusive to the HP group were between SCFA-producing bacteria and commensal bacteria. Examples include interactions of *A. rectalis* with *F. prausnitzii*, *Lachnospira eligens*, and *A. soehngenii*; *E. ramulus* with *C. catus*; *R. bicirculans* with *A. hallii*; and *A. rectalis* with *D. formicigenerans*. However, rewired nodes exclusive to the TA group displayed fewer interactions between SCFA-producing bacteria and commensal bacteria compared with nodes in the HP group. Examples include interactions of *A. rectalis* with *C. catus*. Notably, *S. gallolyticus* was identified as a unique rewired node in the HP dataset, demonstrating interactions with SCFA-producing bacteria and commensal bacteria such as *F. prausnitzii*, *B. faecis*, *B. caecimuris*, *Dysosmobacter* sp000403435, *Anaerotignum lactatifermentans*, and *Amedibacillus dolichus*. These findings suggest that co-occurrence patterns and microbial interactions differ between the HP and TA groups, which could also describe the development of the two colorectal polyp types and their distinct malignancy landscapes.

DISCUSSION

The development of colorectal polyps is significantly influenced by alterations in gut microbiome community composition and ecology. It typically arises from an imbalance in the gut microbiome community and the colonization of microbial species that trigger chronic inflammation, eventually leading to the multistep process of polyp formation[43]. Here, we investigated differences in gut microbiome communities between individuals with and without colorectal polyps, which provided insights concerning the microbial species, functions, and mechanisms that impact colorectal polyp development through the conventional adenoma-carcinoma sequence and the serrated polyp pathway. Furthermore, we identified multiple differentially abundant species in HP patients and TA patients; many of these species have been associated with CRC, dysbiosis, and colorectal adenoma[44-50].

In the present study, the overall gut microbiome compositions did not significantly differ among the CT, HP, and TA groups. However, there were variations in the microbial species associated with each group. These findings are consistent with the results of previous cohort studies that did not demonstrate differences in overall gut microbiome composition between normal samples and samples from patients with adenoma[13,15]. However, previous studies regarding colorectal polyps have yielded inconsistent results regarding community diversity[51,52]. Some studies showed no differences in diversity, whereas others revealed increased diversity in patients with polyps. These discrepancies may be influenced by factors such as sample size, statistical power, or the presence of population-specific microbial drivers or pathogens. Another possible explanation is that the gut microbiome associated with colorectal polyps is similar to the gut microbiome of healthy individuals[52,53]. The discrepancies also may have arisen from the limited taxonomic coverage and reliance on reference genomes during whole metagenomic sequencing taxonomic profiling[54,55].

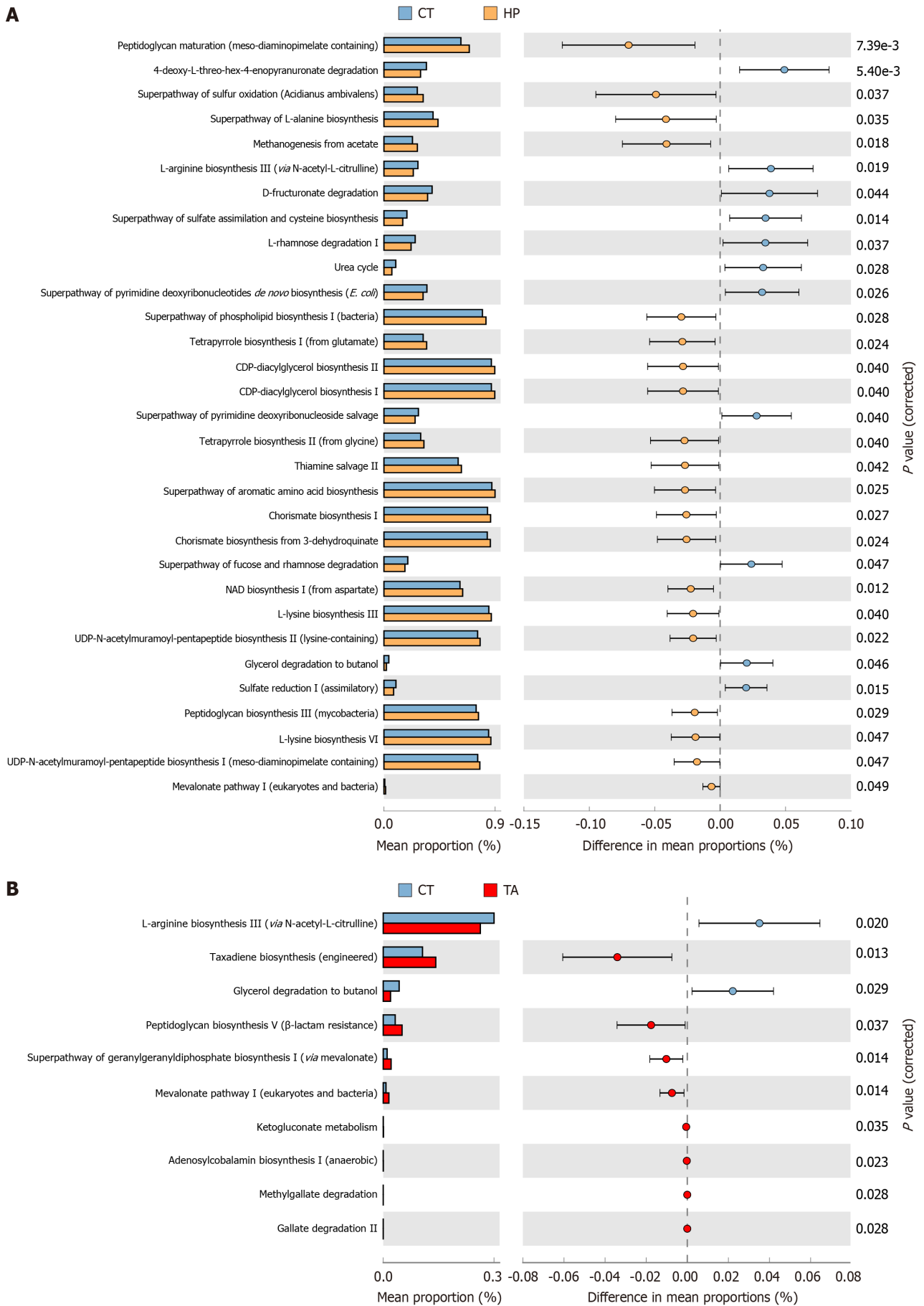


Figure 4 Functional differences in the gut microbiome among control, hyperplastic polyps, and tubular adenoma groups. A: PICRUSt2

demonstrated significant differences in the gut microbiome within MetaCyc pathways between the control (CT) and hyperplastic polyps (HP) groups; B: PICRUSt2 demonstrated significant differences in the gut microbiome within MetaCyc pathways between the CT and tubular adenoma (TA) groups.

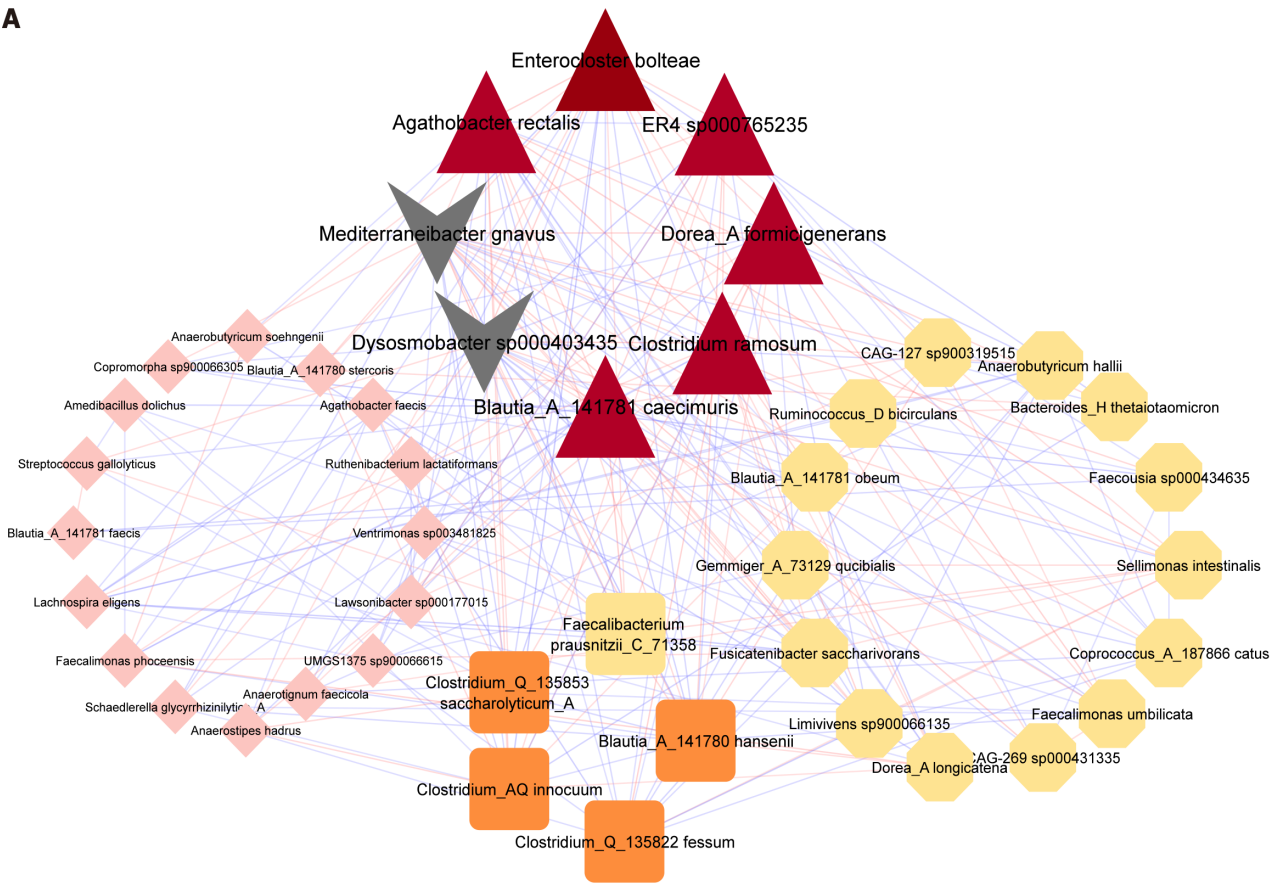
Multiple studies have shown that some pathogenic bacteria, such as *Fusobacterium*, *B. fragilis*, and *E. coli*, are highly abundant in patients with colorectal polyps[4,5,7-9,56]. For example, biofilm formation and virulence factors from *E. coli*, responding to environmental changes in the mucosa, can induce genotoxic effects as well as inflammatory and neoplastic processes. This occurs through the activation of DNA damage, oxidative stress, and the NF- κ B and STAT3 signaling pathways[57]. We did not identify *E. coli* and *Fusobacterium* in the HP and TA groups. These results are consistent with previous findings concerning colorectal adenomas[44,47]. Furthermore, they underscore the importance of developing polyp-specific biomarkers that are specifically associated with colorectal adenomas.

Furthermore, we observed substantial variation in differential microbial species among the HP, TA, and CT groups. The present study revealed a significant increase in *M. gnavus* abundance among HP and TA patients, whereas the abundances of *B. fragilis* and *S. gallolyticus* were only significantly increased in TA patients. *M. gnavus* abundance is elevated in various gastrointestinal diseases, including inflammatory bowel disease, irritable bowel syndrome, CRC, Crohn's disease, and ulcerative colitis[50,58]. This elevated abundance may be associated with inflammation and bowel neoplasia[58]. *M. gnavus* is capable of metabolizing primary bile acids, which are not absorbed by the small intestine, into secondary bile acids[59]. Elevated levels of secondary bile acids can induce oxidative and nitrosative stresses, DNA damage, apoptosis, and mutations in host cells. Furthermore, secondary bile acids interact with the farnesoid X receptor in an antagonist manner, leading to enhanced Wnt signaling in the conventional adenoma-carcinoma sequence[60]. A meta-analysis of case reports and case series from 1970 to 2010 indicated that approximately 60% of patients with *S. gallolyticus* infections also had concurrent colon adenomas or carcinomas, a rate significantly higher than the percentage observed in the general population[61]. Additional studies have shown associations of colorectal adenoma or carcinoma with *S. gallolyticus* infection[62].

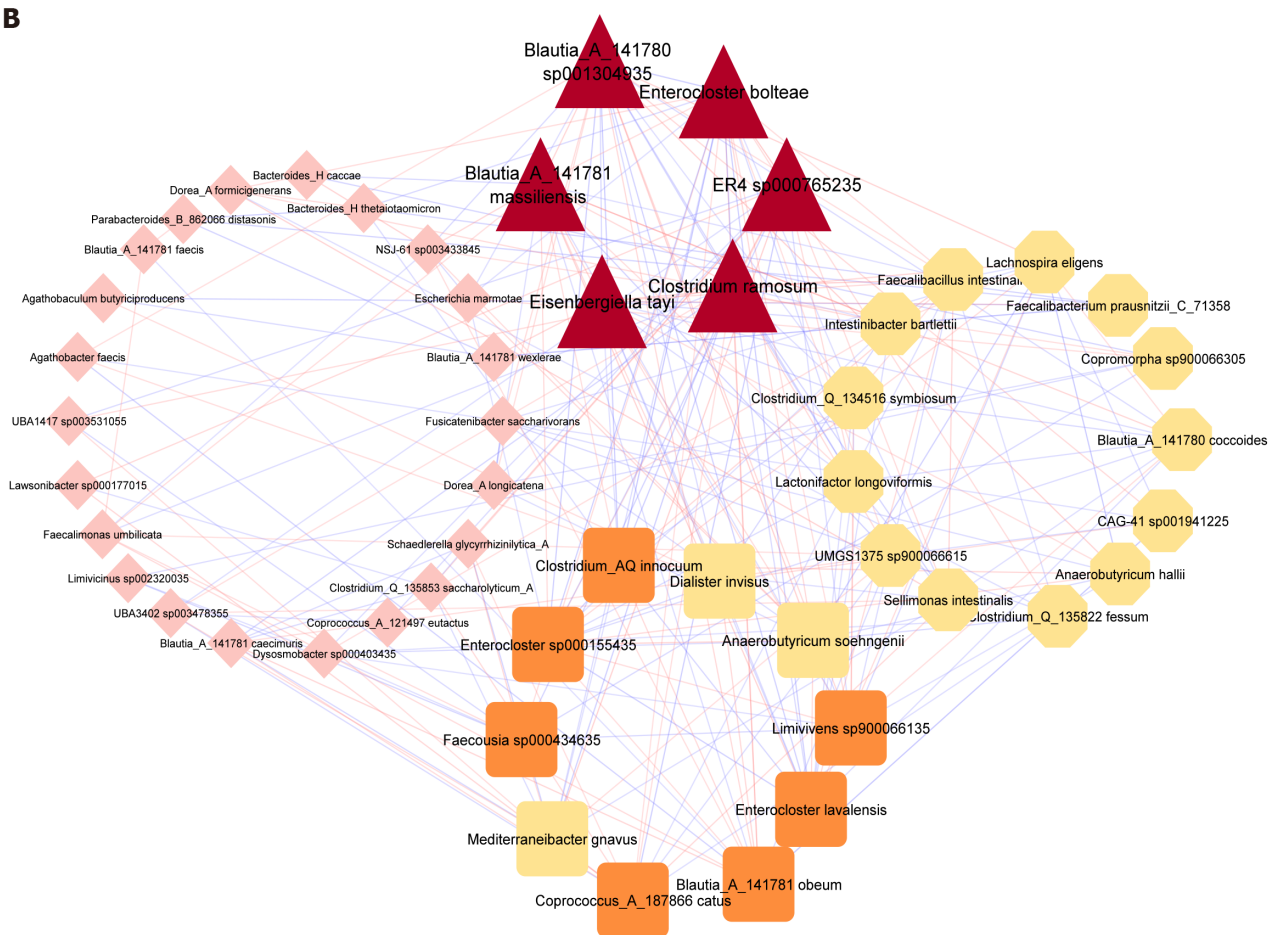
The current study offers additional evidence to support the strong association between *S. gallolyticus* and colorectal adenomas. It has been observed that *S. gallolyticus* is closely linked to the transformation of colorectal mucosa into adenoma, potentially through mechanisms such as epithelial barrier invasion or virulence factor release. *S. gallolyticus* enhances inflammation and tumorigenesis by targeting NF- κ B and Wnt/ β -catenin signaling, upregulating β -catenin levels, and inducing inflammation *via* cytokines (*e.g.*, interleukin-1, interleukin-8, and cyclooxygenase-2)[63-65]. Therefore, *S. gallolyticus* is presumed to participate in neoplastic transformation. Our findings indicate that *S. gallolyticus* is a key contributor to the mevalonate pathway, which is substantially enriched in patients with TA. This pathway plays a crucial role in the biosynthesis of compounds such as isopentenyl pyrophosphate, farnesyl pyrophosphate, and geranylgeranyl pyrophosphate, which serve as building blocks for various essential biomolecules, including lipoproteins, dolichol, ubiquinone, and cholesterol-derived products (*e.g.*, steroid hormones, oxysterols, vitamin D, and bile acids). These metabolites play important roles in the regulation of cellular metabolism[66]. However, isopentenyl pyrophosphate, farnesyl pyrophosphate, and geranylgeranyl pyrophosphate can also contribute to inflammation-mediated tumor growth through oncogenic activation of Ras[66]. Previous studies have revealed that mevalonate pathway inhibition can impede the growth and proliferation of colon cancer cell lines[67]. The present study revealed a novel link between *S. gallolyticus* and the mevalonate pathway, which involved cell signaling in carcinogenesis. Notably, mevalonate pathway activity was predicted to substantially increase in the HP and TA groups compared with the CT group. This finding strongly implies that the mevalonate pathway plays a key role in colorectal polyp formation. Furthermore, the present study revealed significant increases in the abundances of *B. caecimuris*, *C. symbiosum*, and *B. fragilis* among patients with TA. *B. caecimuris* is a commensal bacterium in the human gut, and there is no evidence linking it to colorectal polyps[68]. However, *B. caecimuris* has been detected in fecal samples from CRC patients[69]. The abundance of *C. symbiosum* is increased in colorectal adenoma, making it a promising biomarker for the noninvasive detection of colorectal adenoma[70,71]. *B. fragilis*, a mucin-degrading bacterium[72], can adhere to intestinal mucus and utilize it as a nutrient source for growth[73]. *B. fragilis* produces a metalloprotease that alters signaling pathways and induces the production of reactive oxygen species, resulting in DNA damage and E-cadherin cleavage[74,75]. These results indicated that TA patients predominantly had microbial species associated with inflammation and the adenoma-carcinoma sequence. Our findings highlight the distinct contributions of the gut microbiome to the conventional adenoma-carcinoma sequence and the serrated polyp pathway. In the conventional adenoma-carcinoma sequence, the presence of pathogens and inflammation-enhancing microbial species in an inflammatory environment can promote the development of colorectal carcinogenesis. Our findings also suggest that the microbial species detected in this study may be useful for identifying patients with a high risk of colorectal adenoma.

Functional analysis provides valuable insights into the complex mechanisms underlying the development of serrated polyps. In the present study, we predicted enrichment of the APS reductase pathway in HP patients; this pathway contains a microbial enzyme that metabolizes sulfate to sulfite. Our findings suggest that the APS reductase pathway is associated with SRB, including *D. piger* and *B. wadsworthia*, which can increase H₂S levels. Previous studies concerning gut microbiome alterations among individuals with colorectal adenomas have revealed increased levels of SRB such as *Bilophila*, *Desulfovibrio*, and *B. wadsworthia* in patients with adenomatous polyps[76]. Endogenous production of H₂S primarily occurs through the metabolic activities of SRB and other bacteria, which metabolize inorganic sulfur compounds such as sulfate and sulfite (commonly found in processed food preservatives), as well as organic sulfur compounds (*e.g.*, cysteine or taurine, present in red meat)[77]. There is emerging evidence that the metabolism of organic sulfur by SRB in the human gut may link diets high in red and processed meat to increased risks of early-onset adenomas [78,79]. H₂S can damage the mucosal layer by disrupting disulfide bonds, which causes the mucus layer to become less

A



B



C

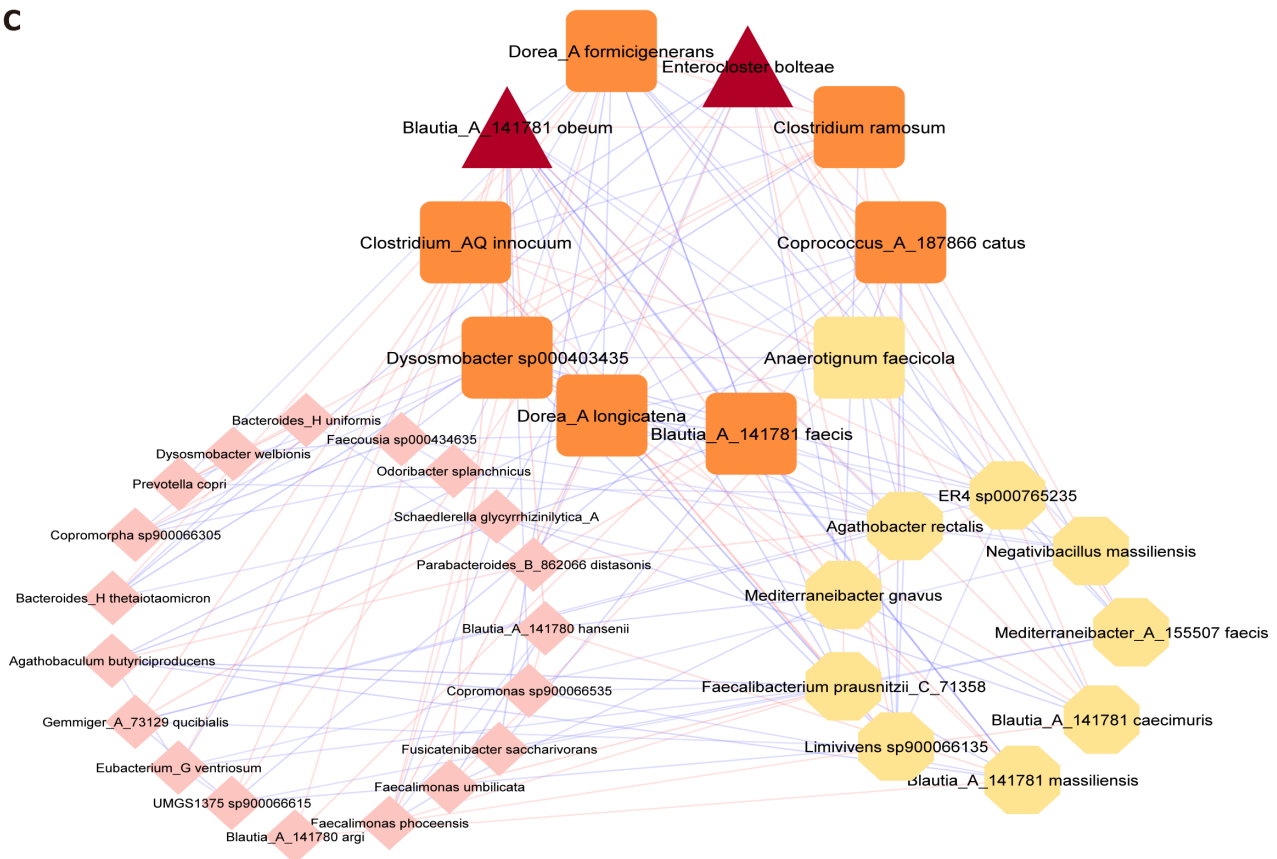


Figure 5 Microbial interaction network of the gut microbiome. A: Co-occurrence networks were constructed at the species level using abundance data from the control (CT) group; B: Co-occurrence networks were constructed at the species level using abundance data from hyperplastic polyps (HP); C: Co-occurrence networks were constructed at the species level using abundance data from tubular adenoma (TA) group. The figure shows that all nodes had more than five connections. Each node in the network represents a single microbial species. The color of each node corresponds to its degree (*i.e.* number of connections with other nodes). Nodes are represented as follows, according to their degree: > 20, red; 16-19, orange; 10-15, yellow; and 6-9, pink. Edges between nodes represent correlations between those nodes; blue indicates a positive correlation, whereas red indicates a negative correlation.

viscous and more permeable. These changes allow toxic compounds and microbial species from the gut lumen to directly interact with the epithelial cell surface, leading to cellular damage, triggering immune responses, and promoting inflammation[79,80]. Chronic inflammation is frequently associated with gastrointestinal cancers, and individuals with colitis have an increased risk of cancer[81]. Therefore, mucin restoration and mucosal barrier strengthening are therapeutic objectives during chronic inflammation, particularly in patients with extensive colitis. This approach is likely to reduce neoplastic processes in the intestinal epithelium and improve health outcomes.

A previous study involving a Thai population revealed decreased *B. thetaiotaomicron* abundance among individuals with adenoma, whereas the abundance was increased among individuals with CRC. Conversely, *P. distasonis* abundance was increased among patients with adenoma and patients with CRC[82]. The present study showed no significant difference in the relative abundances of *B. thetaiotaomicron* and *P. distasonis* between the polyp groups (HP and TA) and the CT group. Both microbial species contribute to thiosulfate oxidation within the sulfur oxidation pathways. Specifically, they are involved in the enzymatic process known as thiosulfate:quinone oxidoreductase, which facilitates thiosulfate oxidation and subsequent tetrathionate production. These intermediates in the sulfur cycle may serve as key sites for electron transfer and energy generation[83]. Nevertheless, it is important to note that the present study specifically focused on the contributions of *B. thetaiotaomicron* and *P. distasonis* to metabolic pathways that exhibited significant differences compared with the CT group, rather than conducting a comprehensive evaluation of all pathways.

Co-occurrence network analysis revealed fewer interactions between beneficial microbial species in the HP and TA groups, which may be associated with the occurrence of colorectal polyps. Notably, positive interactions among beneficial microbial species such as *C. catus*, *Dysosmobacter* sp000403435, and the butyrate-producing genus *Eubacterium* were diminished. Additionally, the HP and TA groups showed fewer negative associations between *C. catus* and opportunistic pathogens such as *E. bolteae*. These results suggest that decreased interactions among beneficial microbial species contribute to colorectal polyp formation. Furthermore, synchronized network analysis demonstrated differences in co-occurrence patterns between the HP and TA groups. For example, the TA group exhibited fewer occurrences of beneficial microbial species compared with the HP group; they also displayed higher levels of co-occurrence involving CRC-associated bacteria. These microbial species are associated with the inflammation that leads to the progression of HP and TA. SCFAs can reduce gut inflammation by promoting gut barrier integrity and permeability through various mechanisms that also help to maintain homeostasis[84-86]. Therefore, the co-occurrence of SCFA-producing bacteria in

(HP) networks; B: The CT and tubular adenoma (TA) networks. Nodes represent microbial species, whereas edges represent correlation coefficients between microbial species. Green edges are only present in the CT network; red nodes and edges are exclusive to the HP and TA groups; and white nodes and gray edges are shared between the CT and HP groups, as well as the CT and TA groups.

patients with HP may enable the maintenance of a good health status[56]. In contrast, a decrease in the co-occurrence of SCFA-producing bacteria, accompanied by an increase in the co-occurrence of CRC-associated bacteria, may be involved in colorectal adenoma formation and colorectal carcinogenesis in TA patients. This hypothesis is supported by a previous report in which patients with cystic fibrosis, who carry adenomas and have a high risk of CRC, exhibited reductions in SCFA-producing bacteria and an increased relative abundance of *B. fragilis*[87].

Colorectal polyps can develop through two main genetic pathways. The conventional adenoma-carcinoma sequence is characterized by mutations in the *adenomatous polyposis coli* gene, chromosomal instability, or microsatellite instability, as well as the absence of CpG island methylator phenotype (CIMP) alterations; this pathway leads to TA. The alternative pathway, the serrated polyp pathway, is mainly characterized by BRAF mutations and high numbers of CIMP alterations; this pathway leads to HP, SSA/Ps, and traditional serrated adenoma. There is substantial histological overlap between SSA/Ps and HP; SSA/Ps constitute up to 30% of all colon cancers. SSA/Ps can develop either as primary tumors or evolve from HP[3], suggesting CRC susceptibility in HP patients. Our investigation of gut microbiome characteristics in different types of colorectal polyps revealed that HP and TA had distinct gut microbiome signatures. This comprehensive analysis of gut microbiome signatures has provided valuable insights concerning gut microbiome contributions to colorectal polyp development, particularly with respect to gut microbiome effects on carcinogenesis. In the serrated polyp pathway, dysbiosis and gastrointestinal disease-associated bacteria, along with the inflammation-inducing sulfur oxidation pathway, contribute to the establishment of a tumor microenvironment. However, this phenomenon is counterbalanced by increased abundances and co-occurrence of SCFA-producing bacteria in HP patients. Furthermore, we speculate that the increased abundance of CRC-associated bacteria mediating the mevalonate pathway involves inflammation and cell proliferation in TA patients, suggesting that such bacteria contribute to the conventional adenoma-carcinoma sequence.

The present study utilized long-read 16S rRNA sequencing, which offers higher resolution for assignments of microbial identity at the species or strain levels. However, it is important to acknowledge the limitations of this study. In particular, it had a small sample size, the results should be confirmed in another cohort, and experimental validation is needed. Furthermore, during bioinformatics analysis, ASVs were aggregated to the species level and then used as input for alpha and beta diversity analyses, as well as differential abundance and co-occurrence analyses.

CONCLUSION

This study utilized differential abundance, co-occurrence, and differential pathway analyses to characterize the gut microbiome signatures in colorectal polyps. The differential abundance analysis identified candidate microbial species that could serve as biomarkers for colorectal polyps. The co-occurrence analysis provided insights concerning the dynamic changes in microbial correlation networks among the CT, HP, and TA groups. The differential pathway analysis predicted functional pathways and determined the roles of microbial species in metabolic function during colorectal polyp development. The results highlight the importance of numerous pathways in colorectal polyp development, offering evidence to support interventions and treatment in the context of CRC carcinogenesis. Furthermore, analyses of the dynamic changes between the CT group and colorectal polyp groups (HP and TA) enhanced the understanding of gut microbiome interactions within the community. Specifically, our findings suggest that HP patients have an increased risk of CRC; more effective strategies are needed to identify and manage such patients.

ACKNOWLEDGEMENTS

In memory of Assistant Professor Dr. Bunchorn Siripongpreeda – his robust leadership and project management made this work possible. We sincerely thank Watsawan Sangkaew, Watcharapol Khoonin, Piangpit Kamolphon, Teeramade Thidseesang, Yanee Poomjaroen, Supanan Makkram, Suyada Sukho, Phaktheema Phoothong, Suchada Panaiem, Chanisara Suebwongdit, Napatsawan Opad, and Tulyawat Prasongmaneerut for assistance with participant recruitment. We especially thank Thanrada Popraros, Napong Leelasithorn, Kawin Chinpong, Tanabhorn Kookongkriksadakorn, Kamonwan Soonklang, Penpisut Homsuwan, and Kerati Jirawattanapalin for assistance with collecting patient information from questionnaires. We also thank Chirayu Auewarakul, Thaniya Sricharunrat, and Montri Gururatsakul for providing medical advice.

FOOTNOTES

Author contributions: Cheevadhanarak S, Sutheworapong S, Thammarongtham C, Intarajak T and Udomchaiprasertkul W contributed to conceptualization; Cheevadhanarak S, Kusonmano K, Intarajak T and Udomchaiprasertkul W contributed to methodology;

Sutheeworapong S, Intarajak T and Khoiri AN contributed to software; Intarajak T, Kittichotirat W and Khoiri AN contributed to validation; Intarajak T and Khoiri AN contributed to formal analysis; Cheevadhanarak S, Intarajak T and Udomchaiprasertkul W contributed to investigation, resources, data curation and writing – original draft preparation; Cheevadhanarak S, Thammarongtham C, Kusonmano K, Khoiri AN, Intarajak T and Udomchaiprasertkul W contributed to writing – review and editing; Intarajak T, contributed to visualization; Cheevadhanarak S, Thammarongtham C, Sutheeworapong S, Kusonmano K and Kittichotirat W contributed to supervision; Intarajak T and Kittichotirat W contributed to project administration and funding acquisition; All authors gave final approval of the version of the article to be published.

Supported by Chulabhorn Royal Academy (Fundamental Fund: Fiscal year 2022 by National Science Research and Innovation Fund), No. FRB650039/0240 Project Code 165422.

Institutional review board statement: The study protocol was reviewed and approved by the Ethical Committee of Chulabhorn Research Institute and the Institutional Review Boards of Chulabhorn Royal Academy (Project Code 045/2563).

Informed consent statement: Informed consent was obtained from all participants involved in the study.

Conflict-of-interest statement: All the authors report no relevant conflicts of interest for this article.

Data sharing statement: Raw sequence data have been deposited in the SRA database under accession number PRJNA940282.

Open-Access: This article is an open-access article that was selected by an in-house editor and fully peer-reviewed by external reviewers. It is distributed in accordance with the Creative Commons Attribution NonCommercial (CC BY-NC 4.0) license, which permits others to distribute, remix, adapt, build upon this work non-commercially, and license their derivative works on different terms, provided the original work is properly cited and the use is non-commercial. See: <https://creativecommons.org/licenses/by-nc/4.0/>

Country of origin: Thailand

ORCID number: Thoranin Intarajak 0000-0001-7756-2528; Wandee Udomchaiprasertkul 0009-0004-6112-4194; Ahmad Nuruddin Khoiri 0000-0003-2883-4149; Sawanee Sutheeworapong 0000-0002-1988-1624; Kanthida Kusonmano 0000-0002-6532-9144; Weerayuth Kittichotirat 0000-0001-8397-633X; Chinae Thammarongtham 0000-0001-5834-4795.

S-Editor: Li L

L-Editor: Filipodia

P-Editor: Zheng XM

REFERENCES

- 1 **Bray F**, Ferlay J, Soerjomataram I, Siegel RL, Torre LA, Jemal A. Global cancer statistics 2018: GLOBOCAN estimates of incidence and mortality worldwide for 36 cancers in 185 countries. *CA Cancer J Clin* 2018; **68**: 394-424 [PMID: 30207593 DOI: 10.3322/caac.21492]
- 2 **Ferlay J**, Colombet M, Soerjomataram I, Mathers C, Parkin DM, Piñeros M, Znaor A, Bray F. Global Cancer Observatory: Cancer Today; 2022. [cited 23 May 2024]. Available from: <https://gco.iarc.fr/today>
- 3 **De Palma FDE**, D'Argenio V, Pol J, Kroemer G, Maiuri MC, Salvatore F. The Molecular Hallmarks of the Serrated Pathway in Colorectal Cancer. *Cancers (Basel)* 2019; **11** [PMID: 31330830 DOI: 10.3390/cancers11071017]
- 4 **Ambrosi C**, Sarshar M, Aprea MR, Pompilio A, Di Bonaventura G, Strati F, Pronio A, Nicoletti M, Zagaglia C, Palamara AT, Scribano D. Colonic adenoma-associated *Escherichia coli* express specific phenotypes. *Microbes Infect* 2019; **21**: 305-312 [PMID: 30763764 DOI: 10.1016/j.micinf.2019.02.001]
- 5 **Xie LL**, Wu N, Zhu YM, Qiu XY, Chen GD, Zhang LM, Liu YL. [Expression of enterotoxigenic *Bacteroides fragilis* and polyketide synthase gene-expressing *Escherichia coli* in colorectal adenoma patients]. *Zhonghua Yi Xue Za Zhi* 2016; **96**: 954-959 [PMID: 27045721 DOI: 10.3760/cma.j.issn.0376-2491.2016.12.010]
- 6 **Kordahi MC**, Stanaway IB, Avril M, Chac D, Blanc MP, Ross B, Diener C, Jain S, McCleary P, Parker A, Friedman V, Huang J, Burke W, Gibbons SM, Willis AD, Darveau RP, Grady WM, Ko CW, DePaolo RW. Genomic and functional characterization of a mucosal symbiont involved in early-stage colorectal cancer. *Cell Host Microbe* 2021; **29**: 1589-1598.e6 [PMID: 34536346 DOI: 10.1016/j.chom.2021.08.013]
- 7 **Little DHW**, Onizuka KM, Khan KJ. Referral for Colonoscopy in Patients with *Streptococcus bovis* Bacteremia and the Association with Colorectal Cancer and Adenomatous Polyps: A Quality Assurance Study. *Gastrointest Disord* 2019; **1**: 385-390 [DOI: 10.3390/gidisord1040031]
- 8 **Hale VL**, Chen J, Johnson S, Harrington SC, Yab TC, Smyrk TC, Nelson H; Boardman LA, Druliner BR, Levin TR, Rex DK, Ahnen DJ, Lance P, Ahlquist DA, Chia N. Shifts in the Fecal Microbiota Associated with Adenomatous Polyps. *Cancer Epidemiol Biomarkers Prev* 2017; **26**: 85-94 [PMID: 27672054 DOI: 10.1158/1055-9965.EPI-16-0337]
- 9 **Liang S**, Mao Y, Liao M, Xu Y, Chen Y, Huang X, Wei C, Wu C, Wang Q, Pan X, Tang W. Gut microbiome associated with APC gene mutation in patients with intestinal adenomatous polyps. *Int J Biol Sci* 2020; **16**: 135-146 [PMID: 31892851 DOI: 10.7150/ijbs.37399]
- 10 **Tsoi H**, Chu ESH, Zhang X, Sheng J, Nakatsu G, Ng SC, Chan AWH, Chan FKL, Sung JY, Yu J. Peptostreptococcus anaerobius Induces Intracellular Cholesterol Biosynthesis in Colon Cells to Induce Proliferation and Causes Dysplasia in Mice. *Gastroenterology* 2017; **152**: 1419-1433.e5 [PMID: 28126350 DOI: 10.1053/j.gastro.2017.01.009]
- 11 **de Vos WM**, Tilg H, Van Hul M, Cani PD. Gut microbiome and health: mechanistic insights. *Gut* 2022; **71**: 1020-1032 [PMID: 35105664 DOI: 10.1136/gutjnl-2021-326789]
- 12 **Rezasoltani S**, Asadzadeh Aghdaei H, Dabiri H, Akhavan Sepahi A, Modarressi MH, Nazemalhosseini Mojarad E. The association between fecal microbiota and different types of colorectal polyp as precursors of colorectal cancer. *Microb Pathog* 2018; **124**: 244-249 [PMID: 30207593]

- 30142468 DOI: [10.1016/j.micpath.2018.08.035](https://doi.org/10.1016/j.micpath.2018.08.035)]
- 13 **Avelar-Barragan J**, DeDecker L, Lu ZN, Coppedge B, Karnes WE, Whiteson KL. Distinct colon mucosa microbiomes associated with tubular adenomas and serrated polyps. *NPJ Biofilms Microbiomes* 2022; **8**: 69 [PMID: [36038569](https://pubmed.ncbi.nlm.nih.gov/36038569/) DOI: [10.1038/s41522-022-00328-6](https://doi.org/10.1038/s41522-022-00328-6)]
 - 14 **Peters BA**, Dominianni C, Shapiro JA, Church TR, Wu J, Miller G, Yuen E, Freiman H, Lustbader I, Salik J, Friedlander C, Hayes RB, Ahn J. The gut microbiota in conventional and serrated precursors of colorectal cancer. *Microbiome* 2016; **4**: 69 [PMID: [28038683](https://pubmed.ncbi.nlm.nih.gov/28038683/) DOI: [10.1186/s40168-016-0218-6](https://doi.org/10.1186/s40168-016-0218-6)]
 - 15 **Yoon H**, Kim N, Park JH, Kim YS, Lee J, Kim HW, Choi YJ, Shin CM, Park YS, Lee DH, Jung HC. Comparisons of Gut Microbiota Among Healthy Control, Patients With Conventional Adenoma, Sessile Serrated Adenoma, and Colorectal Cancer. *J Cancer Prev* 2017; **22**: 108-114 [PMID: [28698865](https://pubmed.ncbi.nlm.nih.gov/28698865/) DOI: [10.15430/JCP.2017.22.2.108](https://doi.org/10.15430/JCP.2017.22.2.108)]
 - 16 **Babraham Bioinformatics**. Software: FastQC [Internet]. 2023. [cited 22 May 2024]. Available from: <https://www.bioinformatics.babraham.ac.uk/projects/fastqc/>
 - 17 **Ewels P**, Magnusson M, Lundin S, Käller M. MultiQC: summarize analysis results for multiple tools and samples in a single report. *Bioinformatics* 2016; **32**: 3047-3048 [PMID: [27312411](https://pubmed.ncbi.nlm.nih.gov/27312411/) DOI: [10.1093/bioinformatics/btw354](https://doi.org/10.1093/bioinformatics/btw354)]
 - 18 **Bolyen E**, Rideout JR, Dillon MR, Bokulich NA, Abnet CC, Al-Ghalith GA, Alexander H, Alm EJ, Arumugam M, Asnicar F, Bai Y, Bisanz JE, Bittinger K, Brejnrod A, Brislawn CJ, Brown CT, Callahan BJ, Carballo-Rodríguez AM, Chase J, Cope EK, Da Silva R, Diener C, Dorrestein PC, Douglas GM, Durall DM, Duvallet C, Edwardson CF, Ernst M, Estaki M, Fouquier J, Gauglitz JM, Gibbons SM, Gibson DL, Gonzalez A, Gorlick K, Guo J, Hillmann B, Holmes S, Holste H, Huttenhower C, Huttley GA, Janssen S, Jarmusch AK, Jiang L, Kaehler BD, Kang KB, Keefe CR, Keim P, Kelley ST, Knights D, Koester I, Kosciorek T, Kreps J, Langille MGI, Lee J, Ley R, Liu YX, Loftfield E, Lozupone C, Maher M, Marotz C, Martin BD, McDonald D, McIver LJ, Melnik AV, Metcalf JL, Morgan SC, Morton JT, Naimey AT, Navas-Molina JA, Nothias LF, Orchanian SB, Pearson T, Peoples SL, Petras D, Preuss ML, Pruesse E, Rasmussen LB, Rivers A, Robeson MS 2nd, Rosenthal P, Segata N, Shaffer M, Shiffer A, Sinha R, Song SJ, Spear JR, Swafford AD, Thompson LR, Torres PJ, Trinh P, Tripathi A, Turnbaugh PJ, Ul-Hasan S, van der Hoof JJJ, Vargas F, Vázquez-Baeza Y, Vogtmann E, von Hippel M, Walters W, Wan Y, Wang M, Warren J, Weber KC, Williamson CHD, Willis AD, Xu ZZ, Zaneveld JR, Zhang Y, Zhu Q, Knight R, Caporaso JG. Reproducible, interactive, scalable and extensible microbiome data science using QIIME 2. *Nat Biotechnol* 2019; **37**: 852-857 [PMID: [31341288](https://pubmed.ncbi.nlm.nih.gov/31341288/) DOI: [10.1038/s41587-019-0209-9](https://doi.org/10.1038/s41587-019-0209-9)]
 - 19 **Callahan BJ**, McMurdie PJ, Rosen MJ, Han AW, Johnson AJ, Holmes SP. DADA2: High-resolution sample inference from Illumina amplicon data. *Nat Methods* 2016; **13**: 581-583 [PMID: [27214047](https://pubmed.ncbi.nlm.nih.gov/27214047/) DOI: [10.1038/nmeth.3869](https://doi.org/10.1038/nmeth.3869)]
 - 20 **McDonald D**, Jiang Y, Balaban M, Cantrell K, Zhu Q, Gonzalez A, Morton JT, Nicolaou G, Parks DH, Karst S, Albertsen M, Hugenholtz P, Desantis T, Song SJ, Bartko A, Havulinna AS, Jousilahti P, Cheng S, Inouye M, Niiranen T, Jain M, Salomaa V, Lahti L, Mirarab S, Knight R. Greengenes2 enables a shared data universe for microbiome studies. 2022 Preprint. Available from: bioRxiv: 520774 [DOI: [10.1101/2022.12.19.520774](https://doi.org/10.1101/2022.12.19.520774)]
 - 21 **McMurdie PJ**, Holmes S. phyloseq: an R package for reproducible interactive analysis and graphics of microbiome census data. *PLoS One* 2013; **8**: e61217 [PMID: [23630581](https://pubmed.ncbi.nlm.nih.gov/23630581/) DOI: [10.1371/journal.pone.0061217](https://doi.org/10.1371/journal.pone.0061217)]
 - 22 **Lahti L**, Shetty S, Blake T, Salojärvi J. Tools for microbiome analysis in R Version 2.1. 26; 2017 [cited 22 May 2023]. Available from: <https://bioconductor.org/packages/release/bioc/html/microbiome.html>
 - 23 **R Core Team**. R: A language and environment for statistical computing [Internet]. 2022. [cited 22 May 2024]. Available from: <https://www.R-project.org/>
 - 24 **Ortiz-Burgos S**. Shannon-Weaver Diversity Index. In: Kennish MJ. Encyclopedia of Estuaries. Dordrecht: Springer Netherlands, 2016: 572-573
 - 25 **Simpson EH**. Measurement of diversity. *Nature* 1949; **163**: 688 [DOI: [10.1038/163688a0](https://doi.org/10.1038/163688a0)]
 - 26 **Chao A**, Chiu CH, Jost L. Phylogenetic diversity measures and their decomposition: a framework based on Hill numbers. In: Pellens R, Grandcolas P. Biodiversity conservation and phylogenetic systematics: preserving our evolutionary heritage in an extinction crisis. Cham: Springer International Publishing, 2016: 141-172
 - 27 **Pielou E**. The measurement of diversity in different types of biological collections. *J Theor Biol* 1966; **13**: 131-144 [DOI: [10.1016/0022-5193\(66\)90013-0](https://doi.org/10.1016/0022-5193(66)90013-0)]
 - 28 **Bray JR**, Curtis JT. An Ordination of the Upland Forest Communities of Southern Wisconsin. *Ecol Monogr* 1957; **27**: 325-349 [DOI: [10.2307/1942268](https://doi.org/10.2307/1942268)]
 - 29 **Pearson K**. LIII. On lines and planes of closest fit to systems of points in space. *Lond, Edinb, and Dublin Philos Mag and J of Sci* 1901; **2**: 559-572 [DOI: [10.1080/14786440109462720](https://doi.org/10.1080/14786440109462720)]
 - 30 **Cao Y**, Dong Q, Wang D, Zhang P, Liu Y, Niu C. microbiomeMarker: an R/Bioconductor package for microbiome marker identification and visualization. *Bioinformatics* 2022; **38**: 4027-4029 [PMID: [35771644](https://pubmed.ncbi.nlm.nih.gov/35771644/) DOI: [10.1093/bioinformatics/btac438](https://doi.org/10.1093/bioinformatics/btac438)]
 - 31 **Segata N**, Izard J, Waldron L, Gevers D, Miropolsky L, Garrett WS, Huttenhower C. Metagenomic biomarker discovery and explanation. *Genome Biol* 2011; **12**: R60 [PMID: [21702898](https://pubmed.ncbi.nlm.nih.gov/21702898/) DOI: [10.1186/gb-2011-12-6-r60](https://doi.org/10.1186/gb-2011-12-6-r60)]
 - 32 **Love MI**, Huber W, Anders S. Moderated estimation of fold change and dispersion for RNA-seq data with DESeq2. *Genome Biol* 2014; **15**: 550 [PMID: [25516281](https://pubmed.ncbi.nlm.nih.gov/25516281/) DOI: [10.1186/s13059-014-0550-8](https://doi.org/10.1186/s13059-014-0550-8)]
 - 33 **Wald A**. Tests of statistical hypotheses concerning several parameters when the number of observations is large. *Trans Amer Math Soc* 1943; **54**: 426-482 [DOI: [10.1090/S0002-9947-1943-0012401-3](https://doi.org/10.1090/S0002-9947-1943-0012401-3)]
 - 34 **Watts SC**, Ritchie SC, Inouye M, Holt KE. FastSpar: rapid and scalable correlation estimation for compositional data. *Bioinformatics* 2019; **35**: 1064-1066 [PMID: [30169561](https://pubmed.ncbi.nlm.nih.gov/30169561/) DOI: [10.1093/bioinformatics/bty734](https://doi.org/10.1093/bioinformatics/bty734)]
 - 35 **Shannon P**, Markiel A, Ozier O, Baliga NS, Wang JT, Ramage D, Amin N, Schwikowski B, Ideker T. Cytoscape: a software environment for integrated models of biomolecular interaction networks. *Genome Res* 2003; **13**: 2498-2504 [PMID: [14597658](https://pubmed.ncbi.nlm.nih.gov/14597658/) DOI: [10.1101/gr.1239303](https://doi.org/10.1101/gr.1239303)]
 - 36 **Goenawan IH**, Bryan K, Lynn DJ. DyNet: visualization and analysis of dynamic molecular interaction networks. *Bioinformatics* 2016; **32**: 2713-2715 [PMID: [27153624](https://pubmed.ncbi.nlm.nih.gov/27153624/) DOI: [10.1093/bioinformatics/btw187](https://doi.org/10.1093/bioinformatics/btw187)]
 - 37 **Douglas GM**, Maffei VJ, Zaneveld JR, Yurgel SN, Brown JR, Taylor CM, Huttenhower C, Langille MGI. PICRUSt2 for prediction of metagenome functions. *Nat Biotechnol* 2020; **38**: 685-688 [PMID: [32483366](https://pubmed.ncbi.nlm.nih.gov/32483366/) DOI: [10.1038/s41587-020-0548-6](https://doi.org/10.1038/s41587-020-0548-6)]
 - 38 **Caspi R**, Billington R, Ferrer L, Foerster H, Fulcher CA, Keseler IM, Kothari A, Krummenacker M, Latendresse M, Mueller LA, Ong Q, Paley S, Subhraveti P, Weaver DS, Karp PD. The MetaCyc database of metabolic pathways and enzymes and the BioCyc collection of pathway/genome databases. *Nucleic Acids Res* 2016; **44**: D471-D480 [PMID: [26527732](https://pubmed.ncbi.nlm.nih.gov/26527732/) DOI: [10.1093/nar/gkv1164](https://doi.org/10.1093/nar/gkv1164)]

- 39 **Parks DH**, Tyson GW, Hugenholtz P, Beiko RG. STAMP: statistical analysis of taxonomic and functional profiles. *Bioinformatics* 2014; **30**: 3123-3124 [PMID: 25061070 DOI: 10.1093/bioinformatics/btu494]
- 40 **Welch BL**. The generalisation of student's problems when several different population variances are involved. *Biometrika* 1947; **34**: 28-35 [PMID: 20287819 DOI: 10.1093/biomet/34.1-2.28]
- 41 **Wu Y**, Zhuang J, Zhang Q, Zhao X, Chen G, Han S, Hu B, Wu W, Han S. Aging characteristics of colorectal cancer based on gut microbiota. *Cancer Med* 2023; **12**: 17822-17834 [PMID: 37548332 DOI: 10.1002/cam4.6414]
- 42 **Giacomini JJ**, Torres-Morales J, Dewhirst FE, Borisy GG, Mark Welch JL. Site Specialization of Human Oral Veillonella Species. *Microbiol Spectr* 2023; **11**: e0404222 [PMID: 36695592 DOI: 10.1128/spectrum.04042-22]
- 43 **Tjalsma H**, Boleij A, Marchesi JR, Dutilh BE. A bacterial driver-passenger model for colorectal cancer: beyond the usual suspects. *Nat Rev Microbiol* 2012; **10**: 575-582 [PMID: 22728587 DOI: 10.1038/nrmicro2819]
- 44 **Amitay EL**, Werner S, Vital M, Pieper DH, Höfler D, Gierse IJ, Butt J, Balavarca Y, Cuk K, Brenner H. Fusobacterium and colorectal cancer: causal factor or passenger? Results from a large colorectal cancer screening study. *Carcinogenesis* 2017; **38**: 781-788 [PMID: 28582482 DOI: 10.1093/carcin/bgx053]
- 45 **Sobhani I**, Bergsten E, Couffin S, Amiot A, Nebbad B, Barau C, de'Angelis N, Rabot S, Canoui-Poitrine F, Mestivier D, Pédrón T, Khazaie K, Sansonetti PJ. Colorectal cancer-associated microbiota contributes to oncogenic epigenetic signatures. *Proc Natl Acad Sci U S A* 2019; **116**: 24285-24295 [PMID: 31712445 DOI: 10.1073/pnas.1912129116]
- 46 **Yachida S**, Mizutani S, Shiroma H, Shiba S, Nakajima T, Sakamoto T, Watanabe H, Masuda K, Nishimoto Y, Kubo M, Hosoda F, Rokutan H, Matsumoto M, Takamaru H, Yamada M, Matsuda T, Iwasaki M, Yamaji T, Yachida T, Soga T, Kurokawa K, Toyoda A, Ogura Y, Hayashi T, Hatakeyama M, Nakagama H, Saito Y, Fukuda S, Shibata T, Yamada T. Metagenomic and metabolomic analyses reveal distinct stage-specific phenotypes of the gut microbiota in colorectal cancer. *Nat Med* 2019; **25**: 968-976 [PMID: 31171880 DOI: 10.1038/s41591-019-0458-7]
- 47 **Yan Y**, Drew DA, Markowitz A, Lloyd-Price J, Abu-Ali G, Nguyen LH, Tran C, Chung DC, Gilpin KK, Meixell D, Parziale M, Schuck M, Patel Z, Richter JM, Kelsey PB, Garrett WS, Chan AT, Stadler ZK, Huttenhower C. Structure of the Mucosal and Stool Microbiome in Lynch Syndrome. *Cell Host Microbe* 2020; **27**: 585-600.e4 [PMID: 32240601 DOI: 10.1016/j.chom.2020.03.005]
- 48 **Yang J**, Li D, Yang Z, Dai W, Feng X, Liu Y, Jiang Y, Li P, Li Y, Tang B, Zhou Q, Qiu C, Zhang C, Xu X, Feng S, Wang D, Wang H, Wang W, Zheng Y, Zhang L, Wang W, Zhou K, Li S, Yu P. Establishing high-accuracy biomarkers for colorectal cancer by comparing fecal microbiomes in patients with healthy families. *Gut Microbes* 2020; **11**: 918-929 [PMID: 31971861 DOI: 10.1080/19490976.2020.1712986]
- 49 **He T**, Cheng X, Xing C. The gut microbial diversity of colon cancer patients and the clinical significance. *Bioengineered* 2021; **12**: 7046-7060 [PMID: 34551683 DOI: 10.1080/21655979.2021.1972077]
- 50 **Crost EH**, Coletto E, Bell A, Juge N. Ruminococcus gnavus: friend or foe for human health. *FEMS Microbiol Rev* 2023; **47** [PMID: 37015876 DOI: 10.1093/femsre/fuad014]
- 51 **Chen HM**, Yu YN, Wang JL, Lin YW, Kong X, Yang CQ, Yang L, Liu ZJ, Yuan YZ, Liu F, Wu JX, Zhong L, Fang DC, Zou W, Fang JY. Decreased dietary fiber intake and structural alteration of gut microbiota in patients with advanced colorectal adenoma. *Am J Clin Nutr* 2013; **97**: 1044-1052 [PMID: 23553152 DOI: 10.3945/ajcn.112.046607]
- 52 **Feng Q**, Liang S, Jia H, Stadlmayr A, Tang L, Lan Z, Zhang D, Xia H, Xu X, Jie Z, Su L, Li X, Li X, Li J, Xiao L, Huber-Schönauer U, Niederseer D, Xu X, Al-Aama JY, Yang H, Wang J, Kristiansen K, Arumugam M, Tilg H, Datz C, Wang J. Gut microbiome development along the colorectal adenoma-carcinoma sequence. *Nat Commun* 2015; **6**: 6528 [PMID: 25758642 DOI: 10.1038/ncomms7528]
- 53 **Zackular JP**, Rogers MA, Ruffin MT 4th, Schloss PD. The human gut microbiome as a screening tool for colorectal cancer. *Cancer Prev Res (Phila)* 2014; **7**: 1112-1121 [PMID: 25104642 DOI: 10.1158/1940-6207.CAPR-14-0129]
- 54 **Laudadio I**, Fulci V, Stronati L, Carissimi C. Next-Generation Metagenomics: Methodological Challenges and Opportunities. *OMICS* 2019; **23**: 327-333 [PMID: 31188063 DOI: 10.1089/omi.2019.0073]
- 55 **Rausch P**, Rühlemann M, Hermes BM, Doms S, Dagan T, Dierking K, Domin H, Fraune S, von Frieling J, Hentschel U, Heinsen FA, Höppner M, Jahn MT, Jaspers C, Kissoyan KAB, Langfeldt D, Rehman A, Reusch TBH, Roeder T, Schmitz RA, Schulenburg H, Soluch R, Sommer F, Stukenbrock E, Weiland-Bräuer N, Rosenstiel P, Franke A, Bosch T, Baines JF. Comparative analysis of amplicon and metagenomic sequencing methods reveals key features in the evolution of animal metaorganisms. *Microbiome* 2019; **7**: 133 [PMID: 31521200 DOI: 10.1186/s40168-019-0743-1]
- 56 **Mangifesta M**, Mancabelli L, Milani C, Gaiani F, de'Angelis N, de'Angelis GL, van Sinderen D, Ventura M, Turroni F. Mucosal microbiota of intestinal polyps reveals putative biomarkers of colorectal cancer. *Sci Rep* 2018; **8**: 13974 [PMID: 30228361 DOI: 10.1038/s41598-018-32413-2]
- 57 **Yang Y**, Jobin C. Microbial imbalance and intestinal pathologies: connections and contributions. *Dis Model Mech* 2014; **7**: 1131-1142 [PMID: 25256712 DOI: 10.1242/dmm.016428]
- 58 **Welham Z**, Li J, Engel AF, Molloy MP. Mucosal Microbiome in Patients with Early Bowel Polyps: Inferences from Short-Read and Long-Read 16S rRNA Sequencing. *Cancers (Basel)* 2023; **15** [PMID: 37894412 DOI: 10.3390/cancers15205045]
- 59 **Devlin AS**, Fischbach MA. A biosynthetic pathway for a prominent class of microbiota-derived bile acids. *Nat Chem Biol* 2015; **11**: 685-690 [PMID: 26192599 DOI: 10.1038/nchembio.1864]
- 60 **Schatoff EM**, Leach BI, Dow LE. Wnt Signaling and Colorectal Cancer. *Curr Colorectal Cancer Rep* 2017; **13**: 101-110 [PMID: 28413363 DOI: 10.1007/s11888-017-0354-9]
- 61 **Boleij A**, Roelofs R, Danne C, Bellais S, Dramsi S, Kato I, Tjalsma H. Selective antibody response to Streptococcus gallolyticus pilus proteins in colorectal cancer patients. *Cancer Prev Res (Phila)* 2012; **5**: 260-265 [PMID: 22012878 DOI: 10.1158/1940-6207.CAPR-11-0321]
- 62 **Abdulmir AS**, Hafidh RR, Mahdi LK, Al-jeboori T, Abubaker F. Investigation into the controversial association of Streptococcus gallolyticus with colorectal cancer and adenoma. *BMC Cancer* 2009; **9**: 403 [PMID: 19925668 DOI: 10.1186/1471-2407-9-403]
- 63 **Abdulmir AS**, Hafidh RR, Bakar FA. Molecular detection, quantification, and isolation of Streptococcus gallolyticus bacteria colonizing colorectal tumors: inflammation-driven potential of carcinogenesis via IL-1, COX-2, and IL-8. *Mol Cancer* 2010; **9**: 249 [PMID: 20846456 DOI: 10.1186/1476-4598-9-249]
- 64 **Abdulmir AS**, Hafidh RR, Abu Bakar F. The association of Streptococcus bovis/gallolyticus with colorectal tumors: the nature and the underlying mechanisms of its etiological role. *J Exp Clin Cancer Res* 2011; **30**: 11 [PMID: 21247505 DOI: 10.1186/1756-9966-30-11]
- 65 **Kumar R**, Herold JL, Schady D, Davis J, Kopetz S, Martinez-Moczygemba M, Murray BE, Han F, Li Y, Callaway E, Chapkin RS, Dashwood WM, Dashwood RH, Berry T, Mackenzie C, Xu Y. Streptococcus gallolyticus subsp. gallolyticus promotes colorectal tumor development. *PLoS Pathog* 2017; **13**: e1006440 [PMID: 28704539 DOI: 10.1371/journal.ppat.1006440]

- 66 **Waller DD**, Park J, Tsantrizos YS. Inhibition of farnesyl pyrophosphate (FPP) and/or geranylgeranyl pyrophosphate (GGPP) biosynthesis and its implication in the treatment of cancers. *Crit Rev Biochem Mol Biol* 2019; **54**: 41-60 [PMID: 30773935 DOI: 10.1080/10409238.2019.1568964]
- 67 **Gong L**, Xiao Y, Xia F, Wu P, Zhao T, Xie S, Wang R, Wen Q, Zhou W, Xu H, Zhu L, Zheng Z, Yang T, Chen Z, Duan Q. The mevalonate coordinates energy input and cell proliferation. *Cell Death Dis* 2019; **10**: 327 [PMID: 30975976 DOI: 10.1038/s41419-019-1544-y]
- 68 **Maturana JL**, Cárdenas JP. Insights on the Evolutionary Genomics of the *Blautia* Genus: Potential New Species and Genetic Content Among Lineages. *Front Microbiol* 2021; **12**: 660920 [PMID: 33981291 DOI: 10.3389/fmicb.2021.660920]
- 69 **Luu K**, Ye JY, Lagishetty V, Liang F, Hauer M, Sedighian F, Kwaan MR, Kazanjian KK, Hecht JR, Lin AY, Jacobs JP. Fecal and Tissue Microbiota Are Associated with Tumor T-Cell Infiltration and Mesenteric Lymph Node Involvement in Colorectal Cancer. *Nutrients* 2023; **15** [PMID: 36678187 DOI: 10.3390/nu15020316]
- 70 **Xie YH**, Gao QY, Cai GX, Sun XM, Sun XM, Zou TH, Chen HM, Yu SY, Qiu YW, Gu WQ, Chen XY, Cui Y, Sun D, Liu ZJ, Cai SJ, Xu J, Chen YX, Fang JY. Fecal Clostridium symbiosum for Noninvasive Detection of Early and Advanced Colorectal Cancer: Test and Validation Studies. *EBioMedicine* 2017; **25**: 32-40 [PMID: 29033369 DOI: 10.1016/j.ebiom.2017.10.005]
- 71 **Coker OO**, Liu C, Wu WKK, Wong SH, Jia W, Sung JY, Yu J. Altered gut metabolites and microbiota interactions are implicated in colorectal carcinogenesis and can be non-invasive diagnostic biomarkers. *Microbiome* 2022; **10**: 35 [PMID: 35189961 DOI: 10.1186/s40168-021-01208-5]
- 72 **Glover JS**, Ticer TD, Engevik MA. Characterizing the mucin-degrading capacity of the human gut microbiota. *Sci Rep* 2022; **12**: 8456 [PMID: 35589783 DOI: 10.1038/s41598-022-11819-z]
- 73 **Huang JY**, Lee SM, Mazmanian SK. The human commensal *Bacteroides fragilis* binds intestinal mucin. *Anaerobe* 2011; **17**: 137-141 [PMID: 21664470 DOI: 10.1016/j.anaerobe.2011.05.017]
- 74 **Sears CL**, Geis AL, Housseau F. *Bacteroides fragilis* subverts mucosal biology: from symbiont to colon carcinogenesis. *J Clin Invest* 2014; **124**: 4166-4172 [PMID: 25105360 DOI: 10.1172/JCI172334]
- 75 **Wick EC**, Rabizadeh S, Albesiano E, Wu X, Wu S, Chan J, Rhee KJ, Ortega G, Huso DL, Pardoll D, Housseau F, Sears CL. Stat3 activation in murine colitis induced by enterotoxigenic *Bacteroides fragilis*. *Inflamm Bowel Dis* 2014; **20**: 821-834 [PMID: 24704822 DOI: 10.1097/MIB.0000000000000019]
- 76 **Kushkevych I**, Dordević D, Vítězová M. Possible synergy effect of hydrogen sulfide and acetate produced by sulfate-reducing bacteria on inflammatory bowel disease development. *J Adv Res* 2021; **27**: 71-78 [PMID: 33318867 DOI: 10.1016/j.jare.2020.03.007]
- 77 **Kushkevych I**, Cejnar J, Tremel J, Dordević D, Kollar P, Vítězová M. Recent Advances in Metabolic Pathways of Sulfate Reduction in Intestinal Bacteria. *Cells* 2020; **9** [PMID: 32178484 DOI: 10.3390/cells9030698]
- 78 **Yazici C**, Wolf PG, Kim H, Cross TL, Vermillion K, Carroll T, Augustus GJ, Mutlu E, Tussing-Humphreys L, Braunschweig C, Xicola RM, Jung B, Llor X, Ellis NA, Gaskins HR. Race-dependent association of sulfidogenic bacteria with colorectal cancer. *Gut* 2017; **66**: 1983-1994 [PMID: 28153960 DOI: 10.1136/gutjnl-2016-313321]
- 79 **Nguyen LH**, Cao Y, Hur J, Mehta RS, Sikavi DR, Wang Y, Ma W, Wu K, Song M, Giovannucci EL, Rimm EB, Willett WC, Garrett WS, Izard J, Huttenhower C, Chan AT. The Sulfur Microbial Diet Is Associated With Increased Risk of Early-Onset Colorectal Cancer Precursors. *Gastroenterology* 2021; **161**: 1423-1432.e4 [PMID: 34273347 DOI: 10.1053/j.gastro.2021.07.008]
- 80 **Moon JY**, Kye BH, Ko SH, Yoo RN. Sulfur Metabolism of the Gut Microbiome and Colorectal Cancer: The Threat to the Younger Generation. *Nutrients* 2023; **15** [PMID: 37111185 DOI: 10.3390/nu15081966]
- 81 **Shussman N**, Wexner SD. Colorectal polyps and polyposis syndromes. *Gastroenterol Rep (Oxf)* 2014; **2**: 1-15 [PMID: 24760231 DOI: 10.1093/gastro/got041]
- 82 **Iadsee N**, Chuaypen N, Techawiwattanaboon T, Jinato T, Patcharatrakul T, Malakorn S, Petchlorlian A, Praditpornsilpa K, Patarakul K. Identification of a novel gut microbiota signature associated with colorectal cancer in Thai population. *Sci Rep* 2023; **13**: 6702 [PMID: 37095272 DOI: 10.1038/s41598-023-33794-9]
- 83 **Brito JA**, Sousa FL, Stelter M, Bandejas TM, Vonrhein C, Teixeira M, Pereira MM, Archer M. Structural and functional insights into sulfide:quinone oxidoreductase. *Biochemistry* 2009; **48**: 5613-5622 [PMID: 19438211 DOI: 10.1021/bi9003827]
- 84 **Hatayama H**, Iwashita J, Kuwajima A, Abe T. The short chain fatty acid, butyrate, stimulates MUC2 mucin production in the human colon cancer cell line, LS174T. *Biochem Biophys Res Commun* 2007; **356**: 599-603 [PMID: 17374366 DOI: 10.1016/j.bbrc.2007.03.025]
- 85 **Peng L**, Li ZR, Green RS, Holzman IR, Lin J. Butyrate enhances the intestinal barrier by facilitating tight junction assembly via activation of AMP-activated protein kinase in Caco-2 cell monolayers. *J Nutr* 2009; **139**: 1619-1625 [PMID: 19625695 DOI: 10.3945/jn.109.104638]
- 86 **Silva YP**, Bernardi A, Frozza RL. The Role of Short-Chain Fatty Acids From Gut Microbiota in Gut-Brain Communication. *Front Endocrinol (Lausanne)* 2020; **11**: 25 [PMID: 32082260 DOI: 10.3389/fendo.2020.00025]
- 87 **Baldwin-Hunter BL**, Rozenberg FD, Annavajhala MK, Park H, DiMango EA, Keating CL, Uhlemann AC, Abrams JA. The gut microbiome, short chain fatty acids, and related metabolites in cystic fibrosis patients with and without colonic adenomas. *J Cyst Fibros* 2023; **22**: 738-744 [PMID: 36717332 DOI: 10.1016/j.jcf.2023.01.013]



Published by **Baishideng Publishing Group Inc**
7041 Koll Center Parkway, Suite 160, Pleasanton, CA 94566, USA
Telephone: +1-925-3991568
E-mail: office@baishideng.com
Help Desk: <https://www.f6publishing.com/helpdesk>
<https://www.wjgnet.com>

